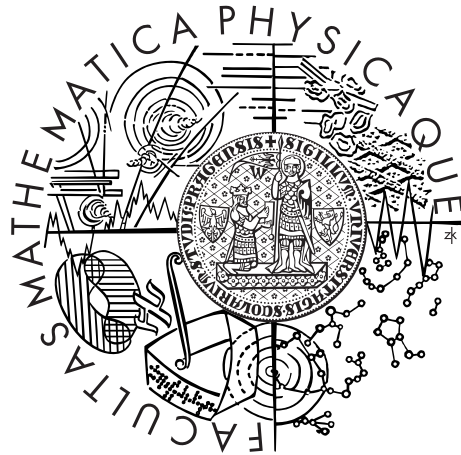


Charles University in Prague
Faculty of Mathematics and Physics

MASTER THESIS



Antonín Koubek

Space–time point processes

Department of Probability and Mathematical Statistics

Supervisor of the master thesis: prof. RNDr. Viktor Beneš, DrSc.

Study programme: Mathematics

Specialization: Probability, Mathematical Statistics and Econometrics

Prague 2013

I thank prof. RNDr. Viktor Beneš, DrSc. for corrections and for supervising of this work.

I declare that I carried out this master thesis independently, and only with the cited sources, literature and other professional sources.

I understand that my work relates to the rights and obligations under the Act No. 121/2000 Coll., the Copyright Act, as amended, in particular the fact that the Charles University in Prague has the right to conclude a license agreement on the use of this work as a school work pursuant to Section 60 paragraph 1 of the Copyright Act.

In on

Author signature

Název práce: Bodové procesy v čase a prostoru

Autor: Antonín Koubek

Katedra: Katedra pravděpodobnosti a matematické statistiky

Vedoucí bakalářské práce: prof. RNDr. Viktor Beneš, DrSc., Katedra pravděpodobnosti a matematické statistiky

Abstrakt: V této práci uvádíme základy teorie bodových procesů v čase a prostoru se zaměřením na prostorovo–časový shot–noise Coxův proces. Dále se z teoretického hlediska zabýváme jeho simulací, posouzením prostorovo–časové separability, jádrovým odhadem funkce intenzity a neparametrickými odhady sumárních statistik s použitím okrajových korekcí. Provádíme numerické výpočty v programu Wolfram Mathematica 9.0 pro dva ambitové a jeden prostorovo–časově separabilní model pomocí uvedené teorie. Pro tyto tři modely určujeme vhodnou šířku pásma pro jádrový odhad funkce intenzity a počítáme také teoretické sumární statistiky včetně párové korelační funkce.

Klíčová slova: ambitový model, shot–noise Coxův proces, odhady, prostorovo–časová separabilita, párová korelační funkce, funkce F .

Title: Point processes in time and space

Author: Antonín Koubek

Department: Department of Probability and Mathematical Statistics

Supervisor of the master thesis: prof. RNDr. Viktor Beneš, DrSc., Department of probability and Mathematical Statistics

Abstract: In this work we present an introduction to the theory of point processes in space and time with focus on space–time shot–noise Cox process. Further from theoretical point of view we study its simulation, space–time separability, kernel estimate of intensity function and non–parametric estimation of some summary statistics using edge corrections. For two ambit models and one space–time separable model we do numerical calculations using the presented theory and software Wolfram Mathematica 9.0. For these three models we do simulations, we select the best bandwidth for kernel estimate of the intensity function and we also calculate some theoretical summary statistics including the pair correlation function.

Keywords: ambit model, shot–noise Cox process, estimation, space–time separability, pair correlation function, function F .

Contents

1	Theoretical background	2
1.1	Point processes on \mathbb{R}^d	2
1.2	Space–time point processes	7
2	Shot–noise Cox processes (SNCP)	10
2.1	Cox point processes	10
2.1.1	Neymann–Scott processes as Cox processes	12
2.2	Space–time SNCP	14
2.3	Three models	17
2.3.1	Model 1 – space–time separable SNCP	19
2.3.2	Model 2, 3 – ambit models	21
3	Simulation algorithms	25
4	Estimation in space–time SNCP	27
4.1	Estimation of intensity function	27
4.2	Second order characteristics	29
5	Numerical results	31
5.1	Theoretical characteristics	33
5.1.1	Calculation of function F for Model 1	34
5.1.2	Calculation of g function for Model 1	36
5.1.3	Calculation of g function for Model 2, 3	38
5.2	Estimation results	39
5.2.1	Intensity estimate	39
5.2.2	Estimation of K and F function	40
	Bibliography	50
	Literature	50
	List of Figures	51
	List of Tables	52

Chapter 1

Theoretical background

Non-formally speaking a point process is a random set of points, i.e. one observation of the point process is a set of points. As an example of a point process we can imagine positions of all people in a town, occurrences of an epidemic in time and space or epicenters of earthquakes. When we have a suitable model for the observations, we can use it to understand their behavior.

This work usually deals with point processes on $\mathbb{R}^2 \times \mathbb{R}_+$, where \mathbb{R}^2 , \mathbb{R}_+ represents space, time respectively. But first of all, let us present some basic theory in \mathbb{R}^d where $d \geq 1, d \in \mathbb{N}$.

1.1 Point processes on \mathbb{R}^d

On \mathbb{R}^d we have a system of Borel subsets \mathcal{B}^d and a system of bounded Borel subsets $\mathcal{B}_0^d \subseteq \mathcal{B}^d$.

Definition 1. (Locally finite subsets and their σ -algebra)

Locally finite subsets of \mathbb{R}^d (point configurations) are elements of $\mathcal{N} = \{\varphi \subseteq \mathbb{R}^d : \varphi(B) < \infty \forall B \in \mathcal{B}_0^d\}$, $\varphi(B)$ denotes the number of points of a set $\varphi \cap B$.

σ -algebra on \mathcal{N} is $\mathfrak{N} = \sigma\{\{\varphi \in \mathcal{N} : \varphi(B) = m\}, m \in \mathbb{N}_0, B \in \mathcal{B}_0^d\}$.

We present the definition of a point process on \mathbb{R}^d , but it is also possible to define point processes on any $S \subseteq \mathcal{B}^d$.

Definition 2. (Point process)

Point process Φ defined on \mathbb{R}^d is a measurable mapping $\Phi : (\Omega, \mathcal{A}, \mathbb{P}) \rightarrow (\mathcal{N}, \mathfrak{N})$, where $(\Omega, \mathcal{A}, \mathbb{P})$ is a probability space, $(\mathcal{N}, \mathfrak{N})$ is a space of point configurations with σ -algebra \mathfrak{N} from the Definition 1.

A point process Φ is called *finite*, when it has finite number of points almost surely.

Note 1. Number of points of the set $\Phi(\omega)$ in a given set $B \in \mathcal{B}^d$ we denote by $\Phi(B)$ where we leave out the variable ω .

Proposition 1. Φ is a point process if and only if $\Phi(B)$ is a random variable for every $B \in \mathcal{B}_0^d$.

Definition 3. (Distribution of a point process)

Distribution of a point process Φ is a measure Π on $(\mathcal{N}, \mathfrak{N})$ defined by $\Pi(\mathcal{U}) = \mathbb{P}(\{\omega \in \Omega : \Phi(\omega) \in \mathcal{U}\})$, $\mathcal{U} \in \mathfrak{N}$.

Definition 4. (Void probabilities)

Let Φ be a point process. By *void probabilities* we understand probabilities $\mathbb{P}(\Phi(B) = 0)$, $B \in \mathcal{B}_0^d$.

Proposition 2. *The distribution of a point process Φ is uniquely determined by its void probabilities.*

Proof. See [3], p.5. □

Definition 5. (Stationarity and Isotropy)

A point process Φ is *stationary* if its distribution is invariant under translations, that is, the distribution of $\Phi + s = \{\xi + s : \xi \in \Phi\}$ is the same as that of Φ for any $s \in \mathbb{R}^d$.

A point process Φ is *isotropic* if its distribution is invariant under rotations about the origin in \mathbb{R}^d , i.e. the distribution of $\mathcal{O}\Phi = \{\mathcal{O}\xi : \xi \in \Phi\}$ is the same as that of Φ for any rotation \mathcal{O} around the origin.

Definition 6. (Intensity measure and Intensity function, Homogeneity)

For a point process Φ we define *intensity measure* by

$$\mu(B) = \mathbb{E}\Phi(B), \quad B \in \mathcal{B}^d,$$

meaning that $\mu(B)$ is a mean number of points of the process Φ in the set B . If there exists a density ρ of the measure μ with respect to Lebesgue measure, that is

$$\mu(B) = \int_B \rho(x)dx, \quad B \in \mathcal{B}^d,$$

then ρ is called *intensity function*.

If ρ is constant, then Φ is said to be *homogeneous* or *first order stationary* with *intensity* ρ .

Definition 7. (Moment measures)

For a point process Φ we define *n-th order moment measure* $\mu^{(n)}$ by

$$\mu^{(n)}(A) = \mathbb{E} \sum_{\xi_1, \dots, \xi_n \in \Phi} I[(\xi_1, \dots, \xi_n) \in A], \quad A \in (\mathcal{B}^d)^n$$

and the *n-th order factorial moment measure* $\alpha^{(n)}$ by

$$\alpha^{(n)}(A) = \mathbb{E} \sum_{\substack{\neq \\ \xi_1, \dots, \xi_n \in \Phi}} I[(\xi_1, \dots, \xi_n) \in A], \quad A \in (\mathcal{B}^d)^n,$$

where \neq over the summation sign means that n points ξ_1, \dots, ξ_n are pairwise distinct.

Note 2. The n -th order moment measure $\mu^{(n)}$ determines the n -th order moments of count variables $\Phi(B)$, $B \subseteq \mathcal{B}^d$, since

$$\mu^{(n)}(B_1 \times \dots \times B_n) = \mathbb{E}[\Phi(B_1) \dots \Phi(B_n)], \quad B_1 \times \dots \times B_n \in \mathcal{B}^d,$$

specially

$$\mu^{(n)}(B \times \dots \times B) = \mathbb{E}[\Phi(B)]^n.$$

In particular we can notice that $\mu = \mu^{(1)} = \alpha^{(1)}$.

Definition 8. (n -th order product density)

If there exists a density $\rho^{(n)}$ of n -th order factorial moment measure $\alpha^{(n)}$ with respect to the nd -dimensional Lebesgue measure, then $\rho^{(n)}$ is called *n -th order product density*.

Note 3. First order product density is the intensity function from the Definition 6, $\rho^{(1)} = \rho$.

Definition 9. (Second order reduced moment measure, Second order intensity reweighted stationarity (SOIRS)).

Suppose that Φ has an intensity function ρ and that the measure

$$\mathcal{K}(B) = \frac{1}{|A|} \mathbb{E} \sum_{\xi, \eta \in \Phi}^{\neq} \frac{I[\xi \in A, \eta - \xi \in B]}{\rho(\xi)\rho(\eta)}, \quad B \in \mathcal{B}^d,$$

does not depend on the choice of $A \in \mathcal{B}^d$ with $0 < |A| < \infty$, where we take $a/0 = 0$ for $a \geq 0$. Then Φ is said to be *second order intensity reweighted stationary* and \mathcal{K} is called the *second order reduced moment measure* (see [1], p.32).

Proposition 3. *If Φ is stationary, then Φ is second order intensity reweighted stationary.*

Proof. *If Φ is stationary, then ρ is constant and*

$$\nu(A) = |A| \rho^2 \mathcal{K}(B) = \mathbb{E} \sum_{\xi, \eta \in \Phi}^{\neq} I[\xi \in A, \eta - \xi \in B]$$

is a translation invariant measure for $A \in \mathcal{B}^d$ when B is fixed, and so ν is proportional to Lebesgue measure on \mathbb{R}^d (see [1], p.32).

□

Definition 10. (K-function)

For a second order intensity reweighted stationary point process Φ we define *K-function* by

$$K(r) = \mathcal{K}(b(0, r)), \quad r \geq 0,$$

where $b(0, r)$ is a d -dimensional sphere with radius r .

Note 4. In the stationary case, $\rho \mathcal{K}(B)$ can be interpreted as the conditional expectation of the number of further points in B given that Φ has a point at the origin.

Definition 11. (Pair correlation function)

If both ρ and $\rho^{(2)}$ exist, the *pair correlation function* is defined by

$$g(\xi, \eta) = \frac{\rho^{(2)}(\xi, \eta)}{\rho(\xi)\rho(\eta)}, \quad \xi, \eta \in \mathbb{R}^d$$

where we take $a/0 = 0$ for $a \geq 0$.

Proposition 4. Let Φ be a SOIRS point process. Then for the pair correlation function g holds

$$g(\xi, \eta) = g(\xi - \eta, 0), \quad \xi, \eta \in \mathbb{R}^d.$$

Note 5. Sometimes we write $g(\xi - \eta)$ instead of $g(\xi - \eta, 0)$ for a SOIRS point process Φ .

Definition 12. (Binomial point process)

Let f be a density function on a set $B \in \mathcal{B}^d$ and let $n \in \mathbb{N}$. A point process Φ consisting of n i.i.d. points with density f is called a *binomial point process* of n points in B with a density f . We write $\Phi \sim \text{binomial}(B, n, f)$.

Definition 13. (Poisson process)

Let ρ be a locally integrable function on \mathbb{R}^d . A point process Φ on \mathbb{R}^d is a *Poisson point process* with intensity function ρ if the following properties are satisfied:

- (i) for any $B \in \mathcal{B}_0^d$, $\Phi(B)$ has a Poisson distribution with parameter $\mu(B)$ (if $\mu(B) = 0$ then $\Phi(B) = 0$),
- (ii) for any $n \in \mathbb{N}$ and $B \in \mathcal{B}_0^d$ with $0 < \mu(B)$, conditional on $\Phi(B) = n$, $\Phi_B = \Phi \cap B \sim \text{binomial}(B, n, f)$ with $f(\xi) = \rho(\xi)/\mu(B)$.

We write $\Phi \sim \text{Poisson}(\mathbb{R}^d, \rho)$.

Note 6. In the Definition 13, (ii) can be replaced by a condition that random variables $\Phi(B_1), \dots, \Phi(B_n)$ are independent for disjoint sets $B_1, \dots, B_n \in \mathcal{B}_0^d$. But (ii) in the Definition 13 gives a better idea how to simulate the process.

Definition 14. (Cluster point process)

Suppose that we have a point process Φ_p (*parent process*) and a set of finite point processes $\{X_u, u \in \mathbb{R}^d\}$. Then

$$X = \bigcup_{\xi \in \Phi_p} X_\xi$$

is called a *cluster point process*. For $\xi \in \Phi_p$, process X_ξ is called a *daughter process*.

Cluster point process X is called a *Poisson cluster point process* when:

- (i) Φ_p is a Poisson point process
- (ii) $X_u, u \in \mathbb{R}^d$, are independent and independent of Φ_p .

Definition 15. (Neymann–Scott process)

Let f be a probability density on \mathbb{R}^d and let X be a Poisson cluster point process. Then X is called a *Neymann–Scott process* if:

- (i) $X_u(\mathbb{R}^d), u \in \mathbb{R}^d$, are i.i.d. random variables,
- (ii) $X_u = \bigcup_{i=1}^{X_u(\mathbb{R}^d)} \eta_i$, where η_i are i.i.d. random vectors with density $f(\cdot - u)$, i.e. points of centered processes $X_u - u$ are i.i.d. with density f .

Definition 16. (Marked point process)

Let Φ be a point process on \mathbb{R}^d , let (M, \mathfrak{M}) be a given measurable space. If a random element $m_\xi : (\Omega, \mathcal{A}, \mathbb{P}) \rightarrow (M, \mathfrak{M})$ is attached to each point $\xi \in \Phi$, then

$$\widehat{\Phi} = \{(\xi, m_\xi) : \xi \in \Phi\}$$

is called a *marked point process* with points in \mathbb{R}^d and mark space M .

If further Φ is a Poisson point process, and conditional on Φ , the marks $\{m_\xi : \xi \in \Phi\}$ are mutually independent, then $\widehat{\Phi}$ is a *marked Poisson process*. If the marks are identically distributed with a common distribution Q , then Q is called the *mark distribution*.

Definition 17. (Independent thinning)

Let Φ be a point process, $p : \mathbb{R}^d \rightarrow [0, 1]$ is a measurable function and

$$\{U(x) : x \in \mathbb{R}^d\}$$

are independent random variables with uniform distribution on $(0, 1)$ and independent of Φ . Point process $\Phi_{th} = \{\xi \in \Phi : U(\xi) < p(\xi)\}$ is called a *thinned point process*.

Proposition 5. For a Poisson point process Φ with intensity measure μ , the corresponding thinned process Φ_{th} is a Poisson point process with intensity measure

$$\mu_{th}(B) = \int_B p(y)\mu(dy), \quad B \in \mathcal{B}^d.$$

Proof. (see also [3], p.18) We are going to show that void probabilities of the thinned process Φ_{th} are equal to void probabilities of a Poisson point process with intensity μ_{th} . Then by the Proposition 2 the proof is finished. For $B \in \mathcal{B}_0^d$ is

$$\begin{aligned} \mathbb{P}(\Phi_{th}(B) = 0) &= \sum_{n=0}^{\infty} \mathbb{P}(\Phi(B) = n) \mathbb{P}(\Phi_{th}(B) = 0 | \Phi(B) = n) \\ &= \sum_{n=0}^{\infty} \frac{\mu(B)^n}{n!} e^{-\mu(B)} \prod_{\xi \in \Phi \cap B} \mathbb{P}(U(\xi) \geq p(\xi) | \Phi(B) = n) \\ &= \sum_{n=0}^{\infty} \frac{\mu(B)^n}{n!} e^{-\mu(B)} \left[\int_0^1 \int_B \mathbb{I}[u \geq p(x)] \frac{\mu(dx)}{\mu(B)} du \right]^n \\ &= \sum_{n=0}^{\infty} \frac{e^{-\mu(B)}}{n!} \left[\int_B (1 - p(x)) \mu(dx) \right]^n \\ &= e^{-\mu(B)} e^{\int_B (1-p(x)) \mu(dx)} = e^{-\int_B p(x) \mu(dx)}. \end{aligned}$$

□

Proposition 6. (Campbell theorem)

For a point process Φ and any non-negative measurable function h it holds that

$$\mathbb{E} \sum_{\xi_1, \dots, \xi_n \in \Phi} h(\xi_1, \dots, \xi_n) = \int_{\mathbb{R}^d} \dots \int_{\mathbb{R}^d} h(x_1, \dots, x_n) \alpha^{(n)}(dx_1, \dots, dx_n)$$

(see [3], p.8).

1.2 Space–time point processes

For our purposes, we will need space–time processes on $\mathbb{R}^3 = \mathbb{R}^2 \times \mathbb{R}_+$, where \mathbb{R}^2 , \mathbb{R}_+ stands for space, time respectively. Sometimes we will also deal with marked point processes with points in \mathbb{R}^3 and mark space \mathbb{R}_+ . According to the Proposition 7 at the end of this chapter, we can view these marked space–time processes as point processes on $\mathbb{R}^3 \times \mathbb{R}_+$, where $\mathbb{R}_+ = (0, \infty)$. Following definitions we formulate in \mathbb{R}^3 , but they can be modified for $\mathbb{R}^3 \times \mathbb{R}_+$ as well.

Similarly as in the Section 1.1, let us have σ –algebra of bounded sets \mathcal{B}_0^3 on \mathbb{R}^3 . Then from the Definition 1 we have *locally finite subsets* of \mathbb{R}^3 given by

$$\mathcal{N} = \{\varphi \subseteq \mathbb{R}^3 : \varphi(B) < \infty \forall B \in \mathcal{B}_0^3\}$$

and by the Definition 2, a *point process* Φ on \mathbb{R}^3 is a random locally finite subset of \mathbb{R}^3 .

We can also define space and time parts of the process Φ that we can use to define space and time parts of summary statistics of Φ .

Definition 18. (Space and time parts).

Let Φ be a space–time point process and suppose that with probability one, $\xi_1 \neq \xi_2$ and $\eta_1 \neq \eta_2$ for any pair of distinct points (ξ_1, η_1) and (ξ_2, η_2) of the process Φ . Then we define

$$\Phi_{space} = \{\xi : (\xi, \eta) \in \Phi\}, \quad \Phi_{time} = \{\eta : (\xi, \eta) \in \Phi\}. \quad (1.1)$$

Intensity measure μ of Φ is by Definition 6

$$\mu(B) = \mathbb{E}\Phi(B), \quad B \in \mathcal{B}^3$$

and if there exists a density ρ on \mathbb{R}^3 with respect to Lebesgue measure then

$$\mu(B) = \int_B \rho(x) dx, \quad B \in \mathcal{B}^3$$

and ρ is called *intensity function*.

Second order intensity measure we define by

$$\alpha^{(2)}(A) = \mathbb{E} \sum_{\substack{\neq \\ \xi_1, \xi_2 \in \Phi}} I[(\xi_1, \xi_2) \in A], \quad A \in (\mathcal{B}^3)^2,$$

which is the second–order factorial moment measure from the Definition 7. If there exists a density $\rho^{(2)}$ of $\alpha^{(2)}$ on $(\mathbb{R}^3)^2$ with respect to 6–dimensional Lebesgue measure then $\rho^{(2)}$ is called *second order intensity function*.

If ρ and $\rho^{(2)}$ both exist then the *pair correlation function* g is, according to the Definition 11,

$$g(\xi, \eta) = \frac{\rho^{(2)}(\xi, \eta)}{\rho(\xi)\rho(\eta)}, \quad \xi, \eta \in \mathbb{R}^3$$

where we take $a/0 = 0$ for $a \geq 0$.

For a second order intensity reweighted stationary point process Φ we define *K-function* (using the Definition 9 and 10) by formula

$$K(r) = \frac{1}{|A|} \mathbb{E} \sum_{\xi, \eta \in \Phi}^{\neq} \frac{I[\xi \in A, \|\eta - \xi\| \leq r]}{\rho(\xi)\rho(\eta)}, \quad r \geq 0$$

for any $A \in \mathcal{B}_0^3$ with positive Lebesgue measure, where $\|\cdot\|$ is an Euclidean norm on \mathbb{R}^3 .

Definition 19. (Space–time separability)

A point process Φ on \mathbb{R}^3 is said to be *first order space–time separable* when

$$\rho(u, t) = \rho_1(u)\rho_2(t), \quad (u, t) \in \mathbb{R}^2 \times \mathbb{R},$$

where ρ_1 and ρ_2 are non–negative functions.

A point process Φ on \mathbb{R}^3 is said to be *second order space–time separable* when

$$g((u, t), (v, s)) = g_1(u, v)g_2(t, s), \quad (u, t), (v, s) \in \mathbb{R}^2 \times \mathbb{R}, \quad (1.2)$$

where g_1 and g_2 are non–negative functions.

Note 7. For a SOIRS point process Φ , (1.2) simplifies (using the Proposition 4) to

$$g(u, t) = g_1(u)g_2(t), \quad (u, t) \in \mathbb{R}^2 \times \mathbb{R}.$$

Note 8. Space–time independence, i.e. independence of u and t for points $\xi = (u, t) \in \Phi$, does not follow from the first order space–time separability. From the first order space–time separability it follows that the intensity measure $\mu(A \times B) = \int_A \rho_1(u)du \int_B \rho_2(t)dt$, $A \in \mathcal{B}^2$, $B \in \mathcal{B}$ is a product measure.

Note 9. We denote ρ_{space} , ρ_{time} the intensity functions of Φ_{space} , Φ_{time} respectively (and similarly for g and K functions). In the case of the first order space–time separability we have

$$\rho_{space}(u) = \rho_1(u) \int_T \rho_2(t)dt, \quad u \in \mathbb{R}^2,$$

$$\rho_{time}(t) = \rho_2(t) \int_W \rho_1(u)du, \quad t \in \mathbb{R}.$$

Definition 20. (Space–time marked point process)

Let Φ be a point process on \mathbb{R}^3 . If a random mark $m_\xi \in \mathbb{R}_+$ is attached to each point $\xi \in \Phi$, then

$$\widehat{\Phi} = \{(\xi, m_\xi) : \xi \in \Phi\}$$

is called a *space–time marked point process* with points in \mathbb{R}^3 and mark space \mathbb{R}_+ .

Proposition 7. *Let Φ be a Poisson process on \mathbb{R}^3 with intensity function $\phi(x)$ and let $\widehat{\Phi} = \{(\xi, m_\xi) : \xi \in \Phi\}$ be a space-time marked Poisson process, where conditional on Φ , each mark m_ξ has a discrete or continuous density p_ξ which does not depend on $\Phi \setminus \xi$. Let $\rho(x, m) = \phi(x)p_x(m)$. Then*

(i) $\widehat{\Phi} \sim \text{Poisson}(\mathbb{R}^3 \times \mathbb{R}_+, \rho)$,

(ii) *if a density on \mathbb{R}_+ defined by $\theta(m) = \int_{\mathbb{R}^3} \rho(x, m) dx$ is locally integrable, then $\{m_\xi : \xi \in \Phi\} \sim \text{Poisson}(\mathbb{R}_+, \theta)$.*

Proof. See [1], p.27.

□

Chapter 2

Shot–noise Cox processes (SNCP)

2.1 Cox point processes

A Cox point process is a generalization of a Poisson point process, where the intensity function is randomized. This provides the process higher variability of the number of points in a selected window.

Definition 21. (Random field on \mathbb{R}^d)

Random field on \mathbb{R}^d is a collection of random variables $Z = \{Z(u) : u \in \mathbb{R}^d\}$ defined on a probability space $(\Omega, \mathcal{A}, \mathbb{P})$.

Definition 22. (Cox point process on \mathbb{R}^d)

Suppose that $Z = \{Z(u) : u \in \mathbb{R}^d\}$ is a non–negative random field so that with probability one, $u \rightarrow Z(u)$ is a locally integrable function. If the conditional distribution of X given Z is a Poisson process on \mathbb{R}^d with intensity function Z , then X is said to be a *Cox point process* driven by Z . The random field Z is called a *driving intensity*.

Note 10. Cox processes are also called *doubly stochastic Poisson processes*.

Definition 23. (Driving measure)

A random measure Λ defined by

$$\Lambda(B) = \int_B Z(u)du, \quad u \in \mathbb{R}^d, B \in \mathcal{B}^d$$

is called a *driving measure* of X .

Note 11. Using the Definition 6 we can calculate the intensity measure μ of X :

$$\mu(B) = \mathbb{E}X(B) = \mathbb{E}[\mathbb{E}(X(B)|\Lambda)] = \mathbb{E}\Lambda(B), \quad B \in \mathcal{B}^d$$

and if $\rho(u) = \mathbb{E}Z(u)$ exists (is finite) and is locally integrable, then $\rho(u) = \mathbb{E}Z(u)$, $u \in \mathbb{R}^d$ is the intensity function of X .

Proposition 8. *Let X be a Cox process on \mathbb{R}^d with a driving intensity $Z(u)$ with finite variance for all $u \in \mathbb{R}^d$. Then the pair correlation function is given by*

$$g(u, v) = \frac{\mathbb{E}[Z(u)Z(v)]}{\mathbb{E}Z(u)\mathbb{E}Z(v)}, \quad u, v \in \mathbb{R}^d.$$

Proof.

$$\begin{aligned} \alpha^{(2)}(B_1 \times B_2) &= \mathbb{E}[X(B_1)X(B_2)] = \mathbb{E}[\mathbb{E}X(B_1)X(B_2)|\Lambda] \\ &= \mathbb{E}[\mathbb{E}[X(B_1)|\Lambda] \mathbb{E}[X(B_2)|\Lambda]], \end{aligned} \quad (2.1)$$

so we obtain

$$\alpha^{(2)}(B_1 \times B_2) = \mathbb{E}[\Lambda(B_1)\Lambda(B_2)] \quad (2.2)$$

for disjoint sets $B_1, B_2 \in \mathcal{B}^d$ where Λ is the driving measure of X and the third equality follows from the Note 6.

Let us denote $(\mathbb{R}^d)^{(2)} = \{(x_1, x_2) : x_i \in \mathbb{R}^d, x_1 \neq x_2\}$ set of all pairs of different points from \mathbb{R}^d . It is an open subset of $(\mathbb{R}^d)^2$. A class of sets

$\{B_1 \times B_2 : B_i \in \mathcal{B}^d, B_1 \cap B_2 = \emptyset\}$ is closed under finite intersections and generates Borel σ -algebra $(\mathcal{B}^d)^{(2)}$ on $(\mathbb{R}^d)^{(2)}$. Since (2.2) holds on this class of sets, it also holds on $(\mathcal{B}^d)^{(2)}$ using Dynkin lemma and because $\alpha^{(2)}$ is equal to zero on $(\mathbb{R}^d)^2 \setminus (\mathbb{R}^d)^{(2)}$, (2.2) holds also on $(\mathbb{R}^d)^2$.

Now when we rewrite (2.2) for densities of Λ and $\alpha^{(2)}$, and use the Definition 11 of the pair correlation function g we are finished with the proof. □

Now we can show, that a Cox process has greater or equal variance of the number of points in a given set compared to a Poisson process with an equal intensity measure.

Proposition 9. *Let X be a Cox process with intensity measure Λ and let Φ be a Poisson process with intensity measure $\mu = \mathbb{E}\Lambda(B)$. Let $B \in \mathcal{B}^d$ with $\text{Var}X(B) < \infty$ and $\text{Var}\Phi(B) < \infty$. Then $\text{Var}X(B) \geq \text{Var}\Phi(B)$.*

Proof. Since $(\mathbb{E}X(B))^2 = \mu(B)^2 = (\mathbb{E}\Phi(B))^2$, we only need to show, that

$$\mathbb{E}(X(B))^2 \geq \mathbb{E}(\Phi(B))^2. \quad (2.3)$$

We can notice from the Definition 7 that $\alpha_X^2(B \times B) = \mathbb{E}X(B)^2 - \mathbb{E}X(B)$ and also $\alpha_\Phi^2(B \times B) = \mathbb{E}\Phi(B)^2 - \mathbb{E}\Phi(B)$. From the proof of the Proposition 8 we know that $\alpha_X^{(2)}(B \times B) = \mathbb{E}\Lambda(B)^2$ and $\alpha_\Phi^{(2)}(B \times B) = \mu(B)^2 = (\mathbb{E}\Lambda(B))^2$. Substituting these results to (2.3) we obtain

$$\alpha_X^{(2)}(B \times B) + \mathbb{E}X(B) \geq \alpha_\Phi^{(2)}(B \times B) + \mathbb{E}\Phi(B)$$

$$\alpha_X^{(2)}(B \times B) \geq \alpha_\Phi^{(2)}(B \times B)$$

$$\mathbb{E}\Lambda(B)^2 \geq (\mathbb{E}\Lambda(B))^2$$

which holds from Jensen inequality and the proof is finished. □

2.1.1 Neymann–Scott processes as Cox processes

In this section we consider those Neymann–Scott processes which are also Cox processes.

Proposition 10. *Let X be a Poisson cluster process on \mathbb{R}^d and let X_u be finite Poisson point processes with intensity functions ρ_u (intensity measures $\mu_u(B) = \int_B \varphi_u(x) dx$ for $B \in \mathcal{B}^d$). Suppose that $Z(u) = \sum_{\xi \in \Phi_p} \varphi_\xi(u)$ is a locally integrable function. Then X is a Cox process with driving intensity Z .*

Proof. For $B \in \mathcal{B}_0^d$ is

$$\begin{aligned} \mathbb{P}(X(B) = 0) &= \mathbb{E} [\mathbb{P}(X(B) = 0 | \Phi_p)] = \mathbb{E} \left[\mathbb{P} \left(\bigcap_{\xi \in \Phi_p} [X_\xi(B) = 0] \mid \Phi_p \right) \right] \\ &= \mathbb{E} \left[\prod_{\xi \in \Phi_p} \mathbb{P}(X_\xi(B) = 0 | \Phi_p) \right] \\ &= \mathbb{E} \left[\prod_{\xi \in \Phi_p} e^{-\mu_\xi(B)} \right] = \mathbb{E} e^{-\sum_{\xi \in \Phi_p} \mu_\xi(B)} = \mathbb{E} e^{-\Lambda(B)}, \end{aligned}$$

which are empty probabilities of a Cox process with driving measure Λ . When we rewrite the result for densities and use the Proposition 2, we are finished with the proof (see [3], p.15–16). □

Next proposition shows, when a Neymann–Scott process is also a Cox process.

Proposition 11. *Let Φ_p be a Poisson process on \mathbb{R}^d with intensity function φ_p . Let $X_u, u \in \mathbb{R}^d$, be independent Poisson processes on \mathbb{R}^d , independent of Φ_p where X_u has intensity function*

$$\varphi_u(x) = \alpha k(x - u)$$

where $\alpha > 0$ is a parameter and k is a probability kernel. Then $X = \cup_{\xi \in \Phi_p} X_\xi$ is a special case of Neymann–Scott process with cluster centers Φ_p and clusters $X_\xi, \xi \in \Phi_p$. Process X is also a Cox process on \mathbb{R}^d driven by

$$Z(u) = \alpha \sum_{\xi \in \Phi_p} k(u - \xi).$$

Proof. It is obvious that $Z(u)$ is a non-negative locally integrable random field and that X is a Poisson cluster process by Definition 14. Using Proposition 10, X is a Cox process with driving intensity $Z(u)$.

Let us verify the definition of Neymann–Scott process (15) for X . $X_u(\mathbb{R}^d), u \in \mathbb{R}^d$ are independent random variables with a Poisson distribution and mean value $\mathbb{E} X_u(\mathbb{R}^d) = \int_{\mathbb{R}^d} \alpha k(x - u) dx = \alpha$ which also implies that processes X_u are almost surely finite. From the definition of Poisson process (13) it follows that the points of the process X_u are independent and identically distributed with density $f_u(x) = \frac{\alpha k(x-u)}{\int_{\mathbb{R}^d} \alpha k(x-u) dx} = k(x - u)$. □

Note 12. In [1], p.61 they only consider a stationary Poisson point process Φ_p .

Note 13. In the general definition of Neymann–Scott process (15), $X_u(\mathbb{R}^d)$ is not restricted to be a Poisson variable. Clearly there also exist more general Cox processes than those that are also Neymann–Scott processes.

Note 14. The intensity function of X is $\rho(u) = \mathbb{E}Z(u) = \alpha\varphi_p(u)$ according to the Campbell theorem.

Definition 24. (Shot–noise Cox process (SNCP))

Let X be a Cox process on \mathbb{R}^d driven by

$$Z(u) = \lambda(u) \sum_{(\xi,r) \in \Phi_p} rk(\xi, u) \quad (2.4)$$

where $k(\cdot, \cdot)$ is a probability kernel function and Φ_p is a Poisson point process on $\mathbb{R}^d \times (0, \infty)$ with a locally integrable intensity function ζ and $\lambda(u)$ is a non–negative bounded function on \mathbb{R}^d . Then X is called a *Shot noise Cox process (SNCP)*.

Note 15. The definition in [1], p. 63 only considers $\lambda(u) = 1, u \in \mathbb{R}^d$. But we need this extension later in our models.

Note 16. In the definition, we suppose a Poisson point process on $\mathbb{R}^d \times (0, \infty)$ which is a measurable subset of \mathbb{R}^{d+1} . As mentioned higher, the definition of a point process can be naturally extended to measurable subsets of \mathbb{R}^{d+1} . Later, we are going to look at a Poisson process on $\mathbb{R}^3 \times (0, \infty)$ as a marked point process with points in \mathbb{R}^3 and marks in $(0, \infty)$.

Note 17. The Definition 24 is implicitly saying (see Definition 22 of a Cox process) that $Z(u)$ is a locally integrable function with probability one. This is satisfied, if the function defined by

$$\rho(u) = \lambda(u) \int_{\mathbb{R}^d \times (0, \infty)} rk(v, u)\zeta(v, r)dvdr, \quad u \in \mathbb{R}^d \quad (2.5)$$

is finite and locally integrable. Then ρ is the intensity function of X (from Campbell theorem).

Example 1. (SNCP as a cluster process)

Let X be a SNCP with driving intensity (2.4). Let $X_{(u,r)}$ be independent Poisson processes, independent of Φ_p with intensity function $\varphi_{(u,r)}(x) = \lambda(u)rk(u, x)$ and define a process $\tilde{X} = \cup_{(\xi,r) \in \Phi_p} X_{(\xi,r)}$. Then \tilde{X} is a Poisson cluster process (see Definition 14), $X_{(u,r)}$ are finite processes and by the Proposition 10, \tilde{X} is a Cox process with driving intensity Z . It means, that X and \tilde{X} have the same distribution and we can view SNCP X as a Poisson cluster process.

Example 2. (SNCP as a Neymann–Scott process)

Let X be a SNCP with driving intensity (2.4). If $\lambda(u) = \alpha$ is constant and Φ_p consists only of points with r coordinate equal to some constant χ , which happens when the intensity function $\zeta(u, r) = \tilde{\zeta}(u)\delta_\chi(r)$, where $\tilde{\zeta}$ is some non–negative locally integrable function on \mathbb{R}^d , then X is a Neymann–Scott process with intensity function $\rho(u) = \alpha\chi\tilde{\zeta}(u)$. We used the fact from Example 1 that we can view X as a Poisson cluster process. In this case, cluster processes $X_{(u,\chi)}$ have intensity function $\alpha\chi k(u, x)$.

Definition 25. (Shot noise G Cox process)

A *shot noise G Cox process* X is an SNCP where the intensity function of Φ_p is

$$\zeta(u, r) = \kappa r^{-\alpha-1} \exp(-\tau r) / \Gamma(1 - \alpha)$$

where $\kappa > 0$, $\alpha < 1$, and $\tau > 0$ (see [1], p.65).

Note 18. The restrictions on parameters are equivalent to local integrability of ζ .

Note 19. The intensity function $\zeta(u, r)$ does not depend on u , which means that Φ_p is stationary under translations of the first coordinate.

Note 20. Intensity function of X is

$$\rho(u) = \lambda(u) \kappa \int_{(0, \infty)} \frac{r^{-\alpha} \exp(-\tau r)}{\Gamma(1 - \alpha)} dr \int_{\mathbb{R}^d} k(x, u) dx = \lambda(u) \kappa \tau^{\alpha-1} \int_{\mathbb{R}^d} k(x, u) dx.$$

Proposition 12. *Let X be a SNCP. If*

$$\beta(u, v) = \lambda(u) \lambda(v) \int \int r^2 k(x, u) k(x, v) \zeta(x, r) dx dr$$

is finite for all $u, v \in \mathbb{R}^d$, then the pair correlation function is given by

$$g(u, v) = 1 + \frac{\beta(u, v)}{\rho(u) \rho(v)}. \quad (2.6)$$

Proof. By the Formula (2.5) and Jensen's inequality $\rho(u)^2 \leq \beta(u, u)$ is finite for all $u \in \mathbb{R}^d$. From (2.4) and (2.5) and Campbell theorem,

$$\begin{aligned} \mathbb{E}[Z(u)Z(v)] &= \mathbb{E} \sum_{(\xi, r), (\xi', r') \in \Phi_p}^{\neq} \lambda(u) r k(\xi, u) \lambda(v) r' k(\xi', v) \\ &\quad + \mathbb{E} \sum_{(\xi, r) \in \Phi_p} \lambda(u) \lambda(v) r^2 k(\xi, u) k(\xi, v) \\ &= \int \int \int \int \lambda(u) r k(\xi, u) \lambda(v) r' k(\xi', v) \zeta(\xi, r) \zeta(\xi', r') d\xi dr d\xi' dr' \\ &\quad + \int \int \lambda(u) \lambda(v) r^2 k(\xi, u) k(\xi, v) \zeta(u, r) du dr \\ &= \rho(u) \rho(v) + \beta(u, v) \end{aligned}$$

which is finite and (2.6) follows from the Definition 11 (see [1], p.67).

□

2.2 Space–time SNCP

In this chapter we present a space–time SNCP, a space–time separable model, two ambit models and their most important characteristics with focus on space–time separability.

Definition 26. (Space–time shot–noise Cox process (SNCP))

Let X be a Cox process on $\mathbb{R}^2 \times \mathbb{R}$ driven by

$$Z(u, t) = \lambda(u, t) \sum_{(\xi, \eta, r) \in \Phi_p} rk((u, t), (\xi, \eta)) \quad (2.7)$$

where $u \in \mathbb{R}^2$, $t \in \mathbb{R}$, $k(\cdot, \cdot)$ is a probability kernel function, Φ_p is a Poisson point process on $\mathbb{R}^2 \times \mathbb{R} \times (0, \infty)$ with locally integrable intensity function ζ and $\lambda(u, t)$ is a non–negative bounded function on $\mathbb{R}^2 \times \mathbb{R}$. Then X is called a *space–time shot noise Cox process (SNCP)*.

Proposition 13. *Let X be a space–time SNCP. Then the intensity function of X is*

$$\rho(u, t) = \lambda(u, t) \int_{\mathbb{R}^2} \int_{\mathbb{R}} \int_{\mathbb{R}_+} rk((u, t), (v, s)) \zeta(v, s, r) dr ds dv \quad (2.8)$$

where $(u, t) \in \mathbb{R}^2 \times \mathbb{R}$.

Proof. From the Definition 6 of the intensity function, $\rho(u, t) = \mathbb{E}Z(u, t)$. The rest follows from the Campbell theorem. □

Example 3. (Space–time SNCP as a cluster process)

Let X be a space–time SNCP. Then we can view the process X as a Poisson cluster process in \mathbb{R}^3 (see Example 1 and the Proposition 10)

$$X = \bigcup_{(\xi, \eta, r) \in \Phi_p} X_{(\xi, \eta, r)}$$

with intensity function of $X_{(\xi, \eta, r)}$

$$\varphi_{(\xi, \eta, r)}(u, t) = \lambda(u, t) rk((u, t), (\xi, \eta)), \quad (u, t) \in \mathbb{R}^2 \times \mathbb{R}. \quad (2.9)$$

The clusters are independent finite Poisson processes because

$$\int_{\mathbb{R}^2} \int_{\mathbb{R}} \varphi_{(\xi, \eta, r)}(u, t) dt du$$

is finite ($\lambda(u, t)$ is a bounded function) for all $(\xi, \eta, r) \in \Phi_p$.

Example 4. (Poisson process Φ_p as a marked Poisson process)

Let Φ_p be a Poisson process on $\mathbb{R}^2 \times \mathbb{R} \times (0, \infty)$ with a locally integrable intensity function ζ . If $\tilde{\zeta}(u, t) = \int_{\mathbb{R}_+} \zeta(u, t, r) dr$ is finite for all $(u, t) \in \mathbb{R}^2 \times \mathbb{R}$ then Φ_p is a marked Poisson point process with points $\Phi \sim \text{Poisson}(\mathbb{R}^2 \times \mathbb{R}, \tilde{\zeta})$ and marks which conditional on Φ are mutually independent with density $p_{(\xi, \eta)}$ of mark $m_{(\xi, \eta)}$ equal to

$$p_{(\xi, \eta)}(r) = \frac{\zeta(\xi, \eta, r)}{\tilde{\zeta}(\xi, \eta)}, \quad r \in (0, \infty)$$

(taking $a/0 = 0$ for $a \geq 0$).

Proposition 14. *Let X be a space–time SNCP with driving intensity Z and intensity function ρ . Then $\rho^{(2)}((u, t), (v, s)) = \mathbb{E}Z(u, v)Z(v, s) = \rho(u, t)\rho(v, s) + \beta((u, t), (v, s))$, where*

$$\beta((u, t), (v, s)) = \lambda(u, t)\lambda(v, s) \int \int \int r^2 k((x, y), (u, t))k((x, y), (v, s))\zeta(x, y, r)dx dy dr.$$

Proof. Follows from the Proposition 12. □

Note 21. We can calculate the pair correlation function g from (2.6):

$$g((u, t), (v, s)) = 1 + \frac{\beta((u, t), (v, s))}{\rho(u, t)\rho(v, s)}, \quad (u, t), (v, s) \in \mathbb{R}^2 \times \mathbb{R}. \quad (2.10)$$

If X is a SOIRS process (see the Definition 9) then by the Proposition 4 the g function depends only on the difference of coordinates of given points in $\mathbb{R}^2 \times \mathbb{R}$, that is $g((u, t), (v, s)) = g((u - v, t - s), 0)$. Then the K function defined in the Definition 10 is

$$K(r, t) = \int_{\mathbb{R}^2 \times \mathbb{R}} I[\|u\| \leq r, |v| \leq t] g(u, v) d(u, v), \quad r > 0, t > 0, \quad (2.11)$$

where $\|u\|$ denotes the Euclidean distance in \mathbb{R}^2 .

Further, it is possible to define space and time parts of g function and K function of the process X by formulas

$$g_1(u) = \frac{1}{|T|^2} \int_T \int_T g(u, t - s) ds dt, \quad u \in \mathbb{R}^2, \quad (2.12)$$

$$g_2(t) = \frac{1}{|W|^2} \int_W \int_W g(u - v, t) du dv, \quad t \in \mathbb{R}, \quad (2.13)$$

$$K_1(r) = \int_{\|u\| \leq r} g_1(u) du, \quad r > 0, \quad (2.14)$$

$$K_2(t) = \int_{-t}^t g_2(s) ds, \quad t > 0. \quad (2.15)$$

We have already defined space–time separability of the intensity function ρ and the g function. At this point we are interested also in space–time separability of kernel k , which is equivalent to space–time independence within the clusters (on condition that $\lambda(u, t)$ is also space–time separable). A useful tool connected with this kind of separability is F function defined as follows:

Definition 27. (Function F)

Let X be a space–time SNCP with K, K_1, K_2 as defined higher. Then function F is defined by formula

$$F(r, t) = \frac{K(r, t) - 2\pi r^2 t}{(K_1(r) - \pi r^2)(K_2(t) - 2t)}, \quad r, t > 0.$$

If the kernel k of the process X is stationary and space–time separable, i.e.

$$k((u, t), (v, s)) = k_2(u - v)k_1(t - s), \quad (2.16)$$

where k_1 is a density on \mathbb{R}^2 and k_2 is a density on \mathbb{R} then the F function from the Definition 27 is a constant depending only on k and intensity of the process Φ_p (see the Section 5.1.1 for the calculation). This property is used for checking space–time separability of k from simulations.

Note 22. If g and K functions are space–time separable then g_{space} , g_{time} , K_{space} and K_{time} functions of processes X_{space} and X_{time} are proportional to g_1 , g_2 , K_1 and K_2 (see [2], p.480). This also explains introducing F function (see also Section 5.1.1).

2.3 Three models

Let us present here three different space–time SNCP models, each of them characterized by some restrictions on the general space–time SNCP, which allows more specific results. Some of the restrictions are common for all the following models:

We consider space–time SNCP X , where:

(i) The Poisson process Φ_p has an intensity function $\zeta(u, t, r) = \nu p(r)$ on $\mathbb{R}^2 \times \mathbb{R} \times \mathbb{R}_+$, where ν is a finite constant and $p(r)$ is a probability density on \mathbb{R}_+ , where we define $p(r) = 0$ for $r \in \mathbb{R}_+ \setminus D(p(r))$, where $D(p(r))$ is the domain of $p(r)$. Since

$$\tilde{\zeta}(u, t) = \int_{\mathbb{R}_+} \zeta(u, t, r) dr = \nu$$

is finite for all $(u, t) \in \mathbb{R}^2 \times \mathbb{R}$, we know (see Example 4) that Φ_p is a marked Poisson point process with points $\Phi \sim \text{Poisson}(\mathbb{R}^2 \times \mathbb{R}, \nu)$ and marks which conditional on Φ are mutually independent with common density p , because

$$\frac{\zeta(\xi, \eta, r)}{\tilde{\zeta}(\xi, \eta)} = \frac{\nu p(r)}{\nu} = p(r), \quad r \in (0, \infty).$$

In this case, Φ is a stationary Poisson point process.

(ii) The kernel k is stationary on $\mathbb{R}^2 \times \mathbb{R}$, i.e. $k((u, t), (v, s)) = k((u-v, t-s), 0)$ for all $(u, t), (v, s) \in \mathbb{R}^2 \times \mathbb{R}$. The interpretation is, that when we move the argument of k to any fixed center, then the value of k depends only on the distance from this center. In the cluster interpretation of SNCP, these centers are points of Φ .

(iii) We observe the process X in a compact set $W \times T \subset \mathbb{R}^2 \times \mathbb{R}$.

Considering this, we obtain new formulations of some of the summary statistics of X . The intensity function of X is (from (2.8))

$$\rho(u, t) = \lambda(u, t) \int_{\mathbb{R}^2} \int_{\mathbb{R}} \int_{\mathbb{R}_+} rk((u, t), (v, s)) \zeta(v, s, r) dr ds dv = \lambda(u, t) \nu \int_{\mathbb{R}_+} rp(r) dr. \quad (2.17)$$

If we adopt the cluster process point of view where points (ξ, η) of Φ determine the centers of the clusters $X_{(\xi, \eta)}$ that are independent Poisson processes, then for every $(\xi, \eta, r) \in \Phi_p$ the intensity function that belongs to a cluster with center (ξ, η) and mark r is (from (2.9))

$$\varphi_{(\xi, \eta, r)}(u, t) = \lambda(u, t) rk((u, t), (\xi, \eta)) = \lambda(u, t) rk(u - \xi, t - \eta), \quad (u, t) \in \mathbb{R}^2 \times \mathbb{R}.$$

Mean number of points of X in the window $W \times T$ is

$$\mathbb{E}X(W \times T) = \int_{W \times T} \rho(u, t) dudt = \nu \int_{\mathbb{R}_+} rp(r) dr \int_{W \times T} \lambda(u, t) dudt. \quad (2.18)$$

Function β (from the Proposition 14) is

$$\begin{aligned} \beta((u, t), (v, s)) &= \lambda(u, t) \lambda(v, s) \\ &\quad \int \int \int r^2 k((x, y), (u, t)) k((x, y), (v, s)) \zeta(x, y, r) dx dy dr \\ &= \nu \lambda(u, t) \lambda(v, s) \\ &\quad \int_{\mathbb{R}_+} r^2 p(r) dr \int_{\mathbb{R}} \int_{\mathbb{R}^2} k(x - u, y - t) k(x - v, y - s) dx dy, \end{aligned} \quad (2.19)$$

The second order product density of X (see the Definition 8) is

$$\begin{aligned} \rho^{(2)}((u, t), (v, s)) &= \mathbb{E}Z(u, t)Z(v, s) = \rho(u, t)\rho(v, s) + \beta((u, t), (v, s)) \\ &= \nu \lambda(u, t) \lambda(v, s) \left[\nu \left(\int_{\mathbb{R}_+} rp(r) dr \right)^2 \right. \\ &\quad \left. + \int_{\mathbb{R}_+} r^2 p(r) dr \int_{\mathbb{R}} \int_{\mathbb{R}^2} k(x - u, y - t) k(x - v, y - s) dx dy \right], \end{aligned} \quad (2.20)$$

and the pair correlation function g we calculate from (2.10):

$$\begin{aligned} g((u, t), (v, s)) &= 1 + \frac{\beta((u, t), (v, s))}{\rho(u, t)\rho(v, s)} \\ &= 1 + \frac{\int_{\mathbb{R}_+} r^2 p(r) dr \int_{\mathbb{R}} \int_{\mathbb{R}^2} k(x - u, y - t) k(x - v, y - s) dx dy}{\nu \left(\int_{\mathbb{R}_+} rp(r) dr \right)^2}, \end{aligned} \quad (2.21)$$

where $(u, t), (v, s) \in \mathbb{R}^2 \times \mathbb{R}$. We can denote

$$h((u, t), (v, s)) = \int_{\mathbb{R}} \int_{\mathbb{R}^2} k(x - u, y - t) k(x - v, y - s) dx dy$$

and using substitution $\tilde{x} = x - u$ and $\tilde{y} = y - t$ we obtain that the function $h((u, t), (v, s)) = \int_{\mathbb{R}} \int_{\mathbb{R}^2} k(\tilde{x}, \tilde{y}) k(\tilde{x} + u - v, \tilde{y} + t - s) d\tilde{x} d\tilde{y}$ is a function of the

difference $u - v$ and $t - s$, so $h((u, t), (v, s)) = \tilde{h}(z, l)$ where $z = u - v$ and $l = t - s$. It follows, that g function is a function of the difference $u - v = z$, $t - s = l$ and we can write

$$g(z, l) = 1 + \frac{\tilde{h}(z, l) \int_{\mathbb{R}_+} r^2 p(r) dr}{\nu \left(\int_{\mathbb{R}_+} r p(r) dr \right)^2},$$

where $\tilde{h}(z, l) = \int_{\mathbb{R}} \int_{\mathbb{R}^2} k(x, y) k(x + z, y + l) dx dy$ and $(z, l) \in \mathbb{R}^2 \times \mathbb{R}$.

It is also possible to calculate the variance $\text{Var } X(B)$ of number of points in a given bounded set $B \in \mathcal{B}_0^3$. We restrict ourselves here to the case when $\lambda(u, t) = 1$, $(u, t) \in \mathbb{R}^2 \times \mathbb{R}$. Using the Definition 7 and (2.20) and (2.17) and the fact that $\alpha_X^{(2)}(B \times B) = \mathbb{E}X(B)^2 - \mathbb{E}X(B)$:

$$\begin{aligned} \text{Var } X(B) &= \alpha_X^{(2)}(B \times B) + \mathbb{E}X(B) - (\mathbb{E}X(B))^2 \\ &= \nu^2 \left(\int_{\mathbb{R}_+} r p(r) dr \right)^2 |B|^2 \\ &\quad + \nu \int_{\mathbb{R}_+} r^2 p(r) dr \int_B \int_B h((u, t), (v, s)) d(u, t) d(v, s) \\ &\quad + \nu \int_{\mathbb{R}_+} r p(r) dr |B| - \nu^2 \left(\int_{\mathbb{R}_+} r p(r) dr \right)^2 |B|^2 \tag{2.22} \\ &= \nu \left(\int_{\mathbb{R}_+} r p(r) dr |B| \right. \\ &\quad \left. + \int_{\mathbb{R}_+} r^2 p(r) dr \int_B \int_B h((u, t), (v, s)) d(u, t) d(v, s) \right), \end{aligned}$$

where $h((u, t), (v, s)) = \int_{\mathbb{R}} \int_{\mathbb{R}^2} k(x - u, y - t) k(x - v, y - s) dx dy$ is as above. Compared to a Poisson process Φ with intensity $\nu \int_{\mathbb{R}_+} r p(r) dr$ (the same intensity as the process X) that has $\text{Var } \Phi(B) = \nu \int_{\mathbb{R}_+} r p(r) dr |B|$ we can see, that $\text{Var } X(B) \geq \text{Var } \Phi(B)$.

2.3.1 Model 1 – space–time separable SNCP

This model is a space–time SNCP X from the Definition 26 satisfying (i)–(iii) from the Section 2.3. Now we present specifications for Model 1:

- (i) Kernel k is space–time separable, i.e.

$$k(u, t) = k_1(u) k_2(t), \quad (u, t) \in \mathbb{R}^2 \times \mathbb{R},$$

where k_1 is a density on \mathbb{R}^2 and k_2 is a density on \mathbb{R} .

- (ii) The deterministic function λ is space–time separable, i.e.

$$\lambda(u, t) = \lambda_1(u) \lambda_2(t), \quad (u, t) \in \mathbb{R}^2 \times \mathbb{R},$$

where λ_1 is a non-negative bounded function on \mathbb{R}^2 and λ_2 is a non-negative bounded function on \mathbb{R} .

(iii) All marks are equal to one with probability one, so we can consider only the process of points Φ instead of Φ_p and use $r = 1$. More formally, this means that the intensity function of Φ_p is

$$\zeta(u, t, r) = \nu \delta_1(r), \quad (u, t, r) \in \mathbb{R}^2 \times \mathbb{R} \times (0, \infty).$$

Now we only rewrite the summary statistics for this model:

Intensity function of X :

$$\rho(u, t) = \nu \lambda(u, t) \int_{\mathbb{R}_+} r p(r) dr = \nu \lambda(u, t), \quad (2.23)$$

intensity function that belongs to a cluster $X_{(\xi, \eta)}$:

$$\varphi_{(\xi, \eta)}(u, t) = \lambda(u, t) k(u - \xi, t - \eta),$$

function beta and second order product density:

$$\begin{aligned} \beta((u, t), (v, s)) &= \nu \lambda(u, t) \lambda(v, s) \\ &\quad \int_{\mathbb{R}_+} r^2 p(r) dr \int_{\mathbb{R}} \int_{\mathbb{R}^2} k(x - u, y - t) k(x - v, y - s) dx dy \\ &= \nu \lambda(u, t) \lambda(v, s) \int_{\mathbb{R}} \int_{\mathbb{R}^2} k(x - u, y - t) k(x - v, y - s) dx dy, \end{aligned} \quad (2.24)$$

$$\begin{aligned} \rho^{(2)}((u, t), (v, s)) &= \nu \lambda(u, t) \lambda(v, s) \left[\nu \left(\int_{\mathbb{R}_+} r p(r) dr \right)^2 \right. \\ &\quad \left. + \int_{\mathbb{R}_+} r^2 p(r) dr \int_{\mathbb{R}} \int_{\mathbb{R}^2} k(x - u, y - t) k(x - v, y - s) dx dy \right] \\ &= \nu \lambda(u, t) \lambda(v, s) \\ &\quad \left(\nu + \int_{\mathbb{R}} \int_{\mathbb{R}^2} k(x - u, y - t) k(x - v, y - s) dx dy \right), \end{aligned} \quad (2.25)$$

and the pair correlation function:

$$\begin{aligned} g((u, t), (v, s)) &= 1 + \frac{\int_{\mathbb{R}_+} r^2 p(r) dr \int_{\mathbb{R}} \int_{\mathbb{R}^2} k(x - u, y - t) k(x - v, y - s) dx dy}{\nu \left(\int_{\mathbb{R}_+} r p(r) dr \right)^2} \\ &= 1 + \frac{\int_{\mathbb{R}} \int_{\mathbb{R}^2} k(x - u, y - t) k(x - v, y - s) dx dy}{\nu}, \end{aligned} \quad (2.26)$$

where $(u, t), (v, s) \in \mathbb{R}^2 \times \mathbb{R}$.

2.3.2 Model 2, 3 – ambit models

Ambit models of space–time Cox point processes are introduced in [4]. Here we consider specially space–time SNCP X from the Definition 26 satisfying (i)–(iii) from the Section 2.3. They do not have the multiplicative structure of k , but instead k is distributed on ambit set $A_u(t) \subset \mathbb{R}^3$. We use the term ambit set in the sense of the following definition:

Definition 28. (Ambit set)

Let (u, t) be a point in \mathbb{R}^3 , let $t_1 > 0$ and $0 < \gamma < \frac{\pi}{2}$ be parameters. Then the *ambit set* $A_u(t)$ on \mathbb{R}^3 is $A_u(t) = \{(v, s) \in \mathbb{R}^2 \times \mathbb{R} : t - t_1 \leq s \leq t, \|v - u\| \leq s \operatorname{tg}(\gamma)\}$.

Note 23. Ambit set is a base–down oriented cone with apex in point (u, t) , base parallel to the plane $s = 0$ and angle γ in the apex (between the vertical line and the surface).

We need to notice, that in ambit models there does not have to be space–time independence of points in a cluster. So the properties of projection processes X_{space} and X_{time} , may not determine the properties of process X .

Example 5. (Non–separability)

Suppose we have an ambit $A_u(t)$ with parameters t_1, γ and uniformly distributed n points on $A_u(t)$ that we denote Y . Then the points of a projection to time Y_{time} are not going to be distributed uniformly.

For both models, k is a density of a uniform distribution on the ambit (k is stationary):

$$k(u - v, t - s) = I[(u - v, t - s) \in A_0(0)] \frac{1}{|A_0(0)|}, \quad (2.27)$$

where $|A_0(0)|$ is a volume of the ambit set $A_0(0)$ (in a sense of three–dimensional Lebesgue measure).

Now we can simplify the function h :

$$\begin{aligned} h((u, t), (v, s)) &= \int_{\mathbb{R}} \int_{\mathbb{R}^2} k((x, y), (u, t)) k((x, y), (v, s)) dx dy \\ &= \int_{\mathbb{R}} \int_{\mathbb{R}^2} k(x - u, y - t) k(x - v, y - s) dx dy \\ &= \frac{|A_u(t) \cap A_v(s)|}{|A_0(0)|^2}, \end{aligned} \quad (2.28)$$

$$(u, t), (v, s) \in \mathbb{R}^2 \times \mathbb{R}.$$

Next two models differ from each other in the distribution of the number of points in one cluster. While in Model 2, mean value of the number of points in one cluster is the same for every cluster, in Model 3 the mean value of number of points in one cluster depends on a mark that is assigned to each cluster and this causes higher variance of number of points in one cluster for Model 3. This has also an effect for example on the pair correlation function that has higher values for Model 3 then for Model 2 in every point of their domain where it is not equal to one.

Model 2

This model is a space–time SNCP X from the Definition 26 satisfying (i)–(iii) from the Section 2.3 and:

(i) Kernel k is a density of a uniform distribution on ambit set defined by (2.27).

(ii) All marks are equal to one with probability one, i.e. the intensity function of Φ_p is

$$\zeta(u, t, r) = \nu \delta_1(r), \quad (u, t, r) \in \mathbb{R}^2 \times \mathbb{R} \times (0, \infty).$$

Intensity function of X :

$$\rho(u, t) = \nu \lambda(u, t) \int_{\mathbb{R}_+} r p(r) dr = \nu \lambda(u, t), \quad (2.29)$$

intensity function that belongs to cluster $X_{(\xi, \eta)}$:

$$\varphi_{(\xi, \eta)}(u, t) = \lambda(u, t) I[(u - \xi, t - \eta) \in A_0(0)] \frac{1}{|A_0(0)|},$$

function beta and second order product density:

$$\begin{aligned} \beta((u, t), (v, s)) &= \nu \lambda(u, t) \lambda(v, s) \int_{\mathbb{R}_+} r^2 p(r) dr \\ &\quad \int_{\mathbb{R}} \int_{\mathbb{R}^2} k((x, y), (u, t)) k((x, y), (v, s)) dx dy \\ &= \nu \lambda(u, t) \lambda(v, s) \int_{\mathbb{R}} \int_{\mathbb{R}^2} k((x, y), (u, t)) k((x, y), (v, s)) dx dy \\ &= \nu \lambda(u, t) \lambda(v, s) \frac{|A_u(t) \cap A_v(s)|}{|A_0(0)|^2}, \end{aligned} \quad (2.30)$$

$$\begin{aligned} \rho^{(2)}((u, t), (v, s)) &= \nu \lambda(u, t) \lambda(v, s) \left[\nu \left(\int_{\mathbb{R}_+} r p(r) dr \right)^2 \right. \\ &\quad \left. + \int_{\mathbb{R}_+} r^2 p(r) dr \int_{\mathbb{R}} \int_{\mathbb{R}^2} k((x, y), (u, t)) k((x, y), (v, s)) dx dy \right] \\ &= \nu \lambda(u, t) \lambda(v, s) \\ &\quad \left(\nu + \int_{\mathbb{R}} \int_{\mathbb{R}^2} k((x, y), (u, t)) k((x, y), (v, s)) dx dy \right) \\ &= \nu \lambda(u, t) \lambda(v, s) \left(\nu + \frac{|A_u(t) \cap A_v(s)|}{|A_0(0)|^2} \right), \end{aligned} \quad (2.31)$$

and the pair correlation function:

$$\begin{aligned}
g((u, t), (v, s)) &= 1 + \frac{\int_{\mathbb{R}_+} r^2 p(r) dr \int_{\mathbb{R}} \int_{\mathbb{R}^2} k((x, y), (u, t)) k((x, y), (v, s)) dx dy}{\nu \left(\int_{\mathbb{R}_+} r p(r) dr \right)^2} \\
&= 1 + \frac{\int_{\mathbb{R}} \int_{\mathbb{R}^2} k((x, y), (u, t)) k((x, y), (v, s)) dx dy}{\nu} \\
&= 1 + \frac{|A_u(t) \cap A_v(s)|}{\nu |A_0(0)|^2},
\end{aligned} \tag{2.32}$$

where $(u, t), (v, s) \in \mathbb{R}^2 \times \mathbb{R}$.

Model 3

This model is a space–time SNCP X from the Definition 26 satisfying (i)–(iii) from the Section 2.3 and:

- (i) Kernel k is a density of a uniform distribution on ambit set defined in (2.27).
- (ii) Distribution of marks is

$$p(r) = \iota \frac{1}{r} e^{-\tau r}, \quad \tau > 0, \epsilon > 0, r \in (\epsilon, \infty),$$

where $\iota = \left(\int_{\epsilon}^{\infty} r^{-1} e^{-\tau r} dr \right)^{-1}$, so the intensity function of Φ_p is

$$\zeta(u, t, r) = \nu \iota \frac{1}{r} e^{-\tau r}, \quad \tau > 0, (u, t, r) \in \mathbb{R}^2 \times \mathbb{R} \times (\epsilon, \infty).$$

Since for $\epsilon = 0$ the integral $\int_{\mathbb{R}_+} p(r) dr$ is not be finite, the process Φ_p would not be a marked Poisson point process (the intensity function $\tilde{\zeta}(u, t)$ of Φ is not locally integrable) for $r \in (0, \infty)$. For this reason we choose $\epsilon > 0$ small and define $p(r)$ only for $r \in (\epsilon, \infty)$.

The distribution $p(r)$ corresponds to G Cox process with $\alpha = 0$ and $\kappa = \nu \iota$ from the Definition 25.

Intensity function of X :

$$\rho(u, t) = \nu \lambda(u, t) \int_{(\epsilon, \infty)} r p(r) dr = \nu \iota \lambda(u, t) \frac{e^{-\tau \epsilon}}{\tau}, \tag{2.33}$$

intensity function that belongs to cluster $X_{(\xi, \eta)}$:

$$\varphi_{(\xi, \eta)}(u, t) = \lambda(u, t) I[(u - \xi, t - \eta) \in A_0(0)] \frac{1}{|A_0(0)|},$$

function beta and second order product density:

$$\begin{aligned}
\beta((u, t), (v, s)) &= \nu \lambda(u, t) \lambda(v, s) \int_{(\epsilon, \infty)} r^2 p(r) dr \\
&\quad \int_{\mathbb{R}} \int_{\mathbb{R}^2} k((x, y), (u, t)) k((x, y), (v, s)) dx dy \\
&= \nu \lambda(u, t) \lambda(v, s) e^{-\tau \epsilon} \frac{1 + \epsilon \tau}{\tau^2} \\
&\quad \int_{\mathbb{R}} \int_{\mathbb{R}^2} k((x, y), (u, t)) k((x, y), (v, s)) dx dy \\
&= \nu \lambda(u, t) \lambda(v, s) e^{-\tau \epsilon} \frac{1 + \epsilon \tau}{\tau^2} \frac{|A_u(t) \cap A_v(s)|}{|A_0(0)|^2},
\end{aligned} \tag{2.34}$$

$$\begin{aligned}
\rho^{(2)}((u, t), (v, s)) &= \nu \lambda(u, t) \lambda(v, s) \left[\nu \left(\int_{(\epsilon, \infty)} r p(r) dr \right)^2 \right. \\
&\quad \left. + \int_{(\epsilon, \infty)} r^2 p(r) dr \int_{\mathbb{R}} \int_{\mathbb{R}^2} k((x, y), (u, t)) k((x, y), (v, s)) dx dy \right] \\
&= \nu \lambda(u, t) \lambda(v, s) \frac{\nu e^{-\tau \epsilon}}{\tau^2} \left(\nu \nu e^{-\epsilon \tau} \right. \\
&\quad \left. + (1 + \epsilon \tau) \int_{\mathbb{R}} \int_{\mathbb{R}^2} k((x, y), (u, t)) k((x, y), (v, s)) dx dy \right) \\
&= \nu \lambda(u, t) \lambda(v, s) \frac{\nu e^{-\tau \epsilon}}{\tau^2} \left(\nu \nu e^{-\epsilon \tau} + (1 + \epsilon \tau) \frac{|A_u(t) \cap A_v(s)|}{|A_0(0)|^2} \right),
\end{aligned} \tag{2.35}$$

and the pair correlation function:

$$\begin{aligned}
g((u, t), (v, s)) &= 1 + \frac{\int_{\mathbb{R}_+} r^2 p(r) dr \int_{\mathbb{R}} \int_{\mathbb{R}^2} k((x, y), (u, t)) k((x, y), (v, s)) dx dy}{\nu \left(\int_{\mathbb{R}_+} r p(r) dr \right)^2} \\
&= 1 + \frac{1 + \epsilon \tau}{\nu \nu e^{-\epsilon \tau}} \int_{\mathbb{R}} \int_{\mathbb{R}^2} k((x, y), (u, t)) k((x, y), (v, s)) dx dy \\
&= 1 + \frac{1 + \epsilon \tau}{\nu \nu e^{-\epsilon \tau}} \frac{|A_u(t) \cap A_v(s)|}{|A_0(0)|^2},
\end{aligned} \tag{2.36}$$

where $(u, t), (v, s) \in \mathbb{R}^2 \times \mathbb{R}$.

Chapter 3

Simulation algorithms

Here we present an algorithm for simulating realizations of a space–time SNCP X from the Definition 26 satisfying (i)–(iii) from the Section 2.3 in a window $W \times T$. We interpret the process X with intensity function

$$\rho(u, t) = \lambda(u, t) \nu \int_{(0, \infty)} rp(r) dr, \quad (u, t) \in \mathbb{R}^2 \times \mathbb{R} \quad (3.1)$$

as a cluster point process

$$X = \bigcup_{(\xi, \eta, r) \in \Phi_p} X_{(\xi, \eta, r)}$$

(see Example 1) consisting of clusters $X_{(\xi, \eta, r)}$, $(\xi, \eta, r) \in \Phi_p$ with intensity function

$$\varphi_{(\xi, \eta, r)}(u, t) = \lambda(u, t) rk(u - \xi, t - \eta), \quad (u, t) \in \mathbb{R}^2 \times \mathbb{R}.$$

To reduce edge effects, we use a larger window \bar{W} , $W \times T \subset \bar{W}$ and after the simulation we cut the pattern to $W \times T$. The idea behind this is that the distribution of points in one cluster may not be bounded so there is a non–zero probability that we observe a point of X inside $W \times T$ even from very distant cluster center $X_{(u, t, r)}$. We need to set \bar{W} large enough to cover all the possible cluster centers that have some significant probability to contribute with a point to $X \cap (W \times T)$.

Note 24. The algorithm may work only approximately for some kernels k . But using adequate parameters during the simulation one can obtain almost exact results.

Algorithm:

- (i) Generate a realization of a Poisson point process

$$\Phi_p \sim \text{Poisson}(\mathbb{R}^2 \times \mathbb{R} \times (0, \infty), \nu p(r)).$$

We interpret this process as a marked Poisson point process (see Example 4) with points $\Phi \sim \text{Poisson}(\mathbb{R}^2 \times \mathbb{R}, \nu)$ and marks $m_{(u, t)}$ with distribution p . This is done in two steps:

- a) Generate a realization of a stationary Poisson process Φ with intensity ν in the window \bar{W} . This is done by generating a Poisson distributed number with

mean value $\hat{\nu} = \nu |\bar{W}|$ that determines number of points of Φ in \bar{W} and then, given this number, all $\hat{\nu}$ points are uniformly and independently of the other points distributed in \bar{W} .

b) Generate a mark $m_{(\xi,\eta)}$ from distribution p for every point $(\xi, \eta) \in \Phi$. By now, we are able to construct the marked Poisson process Φ_p :

$$\Phi_p = \{(\xi, \eta, m_{(\xi,\eta)}) : (\xi, \eta) \in \Phi\}.$$

(ii) For each $(\xi, \eta, r) \in \Phi_p$ generate a Poisson process with intensity function

$$\varphi_{(\xi,\eta,r)}(u, t) = \lambda(u, t)rk(u - \xi, t - \eta), \quad (u, t) \in \mathbb{R}^2 \times \mathbb{R}.$$

This is done in three steps:

a) For each $(\xi, \eta, r) \in \Phi_p$ generate a stationary Poisson process $C_{(\xi,\eta,r)}^m$ in $W_C(\Delta) \cap (W \times T)$, where $W_C(\Delta) = ([\xi_1 - \Delta_x, \xi_1 + \Delta_x] \times [\xi_2 - \Delta_y, \xi_2 + \Delta_y] \times [\eta - \Delta_{z_d}, \eta + \Delta_{z_u}])$, $(\xi_1, \xi_2) = \xi$ and $\Delta = (\Delta_x, \Delta_y, \Delta_{z_d}, \Delta_{z_u})$ is selected so that the set $W_C(\Delta)$ covers all points of the cluster $X_{(\xi,\eta,r)}$ with high probability, with intensity

$$\varphi_{(\xi,\eta,r)}^M = \lambda_m rk_m,$$

where λ_m is upper bound for λ on \bar{W} and k_m is upper bound for k on \bar{W} so it holds that $\lambda_m \geq \lambda_{(v,s)}(u, t)$ for every $(v, s), (u, t) \in \bar{W}$. We can notice, that in this step we are also cutting the pattern to $W \times T$ to make the simulation computationally faster.

b) (First independent thinning)

For each point (u, t) in $C_{(\xi,\eta,r)}^m$ and each $(\xi, \eta, r) \in \Phi_p$ do independent thinning (see the Proposition 5) with retention probability

$$q(u, t) = \frac{k(u - \xi, t - \eta)}{k_m}.$$

By this we obtain a process X^m with intensity $\rho_m = \lambda_m \nu \int_{(0,\infty)} rp(r)dr$ that is formed by clusters $C_{(\xi,\eta,r)} \sim \text{Poisson}(W \times T, \lambda_m rk(u - \xi, t - \eta))$.

c) (Second independent thinning)

Independent thinning with retention probability

$$p(u, t) = \frac{\lambda(u, t)}{\lambda_m}$$

for each point $(u, t) \in X^m$. By this we obtain process X with intensity function (3.1) formed by clusters $X_{(\xi,\eta,r)} \sim \text{Poisson}(W \times T, \lambda rk(u - \xi, t - \eta))$ which we desired.

Note 25. Some clusters $X_{(\xi,\eta,r)}$ may be empty if they contain no points in $W \times T$.

Examples of realizations of the process X for Model 1, 2, 3 are in the Figure 5.1.

Chapter 4

Estimation in space–time SNCP

Suppose we are given one or generally n realizations R_j , $j = 1 \dots n$ of a space–time process X in a compact window $W \times T \subset \mathbb{R}^3$. A realization R_j consists of points (u_i^j, t_i^j) , $i = 1 \dots N_{R_j}$, $(u_i^j, t_i^j) \in W \times T$, N_{R_j} is the number of points of the realization inside $W \times T$. We would like to estimate some first and second order characteristics of X with focus on the intensity function and K –function. We are also interested in the question whether the process X has space–time separable kernel k (see (2.16)). For this purpose we also estimate function F .

The method consists in calculating the characteristics from every realization separately and then calculating an average of these n results. This is how we estimate the intensity function. Estimation of K , K_1 and K_2 functions requires a previous knowledge of the intensity function. We can either use the theoretical value or a previously estimated value and then we use the method as before. In the estimation of F function we only use previously calculated estimates.

Usually the calculations for a continuous variable would be computationally too slow, so we use some natural discretization D of the window $W \times T$. The described algorithm has a general part that does not suppose anything more specific about the process, so it is applicable for any space–time point process, and a modification that is useful in case of first order space–time separability of the process.

4.1 Estimation of intensity function

We would like to estimate the intensity function $\rho(u, t)$, $(u, t) \in W \times T$. If we suppose that the process X is first order space–time separable (see the Definition 19), then

$$\rho(u, t) = \rho_1(u)\rho_2(t) = \frac{\rho_{space}(u)}{\int_T \rho_2(t)dt} \frac{\rho_{time}(t)}{\int_W \rho_1(u)du} = \frac{\rho_{space}(u)\rho_{time}(t)}{\int_{W \times T} \rho(u,t)dudt} = \frac{\rho_{space}(u)\rho_{time}(t)}{N},$$

where $(u, t) \in W \times T$ and N is the expected number of points in $W \times T$. We can estimate separately the space part ρ_{space} and the time part ρ_{time} and then the intensity estimate is

$$\widehat{\rho}(u, t) = \frac{\widehat{\rho}_{space}(u)\widehat{\rho}_{time}(t)}{N}, \quad (u, t) \in W \times T,$$

where N is the expected number of points in $W \times T$.

For the estimation from a given realization R_l of the process X we use kernel method with edge corrections:

$$\hat{\rho}_{space}^l(u) = \sum_{i=1}^{N_{R_l}} \frac{\omega_b(u - u_i^l)}{c_{W,b}(u_i^l)}, \quad u \in W, \quad (4.1)$$

where N_{R_l} is the number of points of the realization R_l , $\omega_b(u) = \omega(\frac{u}{b})\frac{1}{b^2}$ is a probability kernel in \mathbb{R}^2 with bandwidth $b > 0$. Here ω is a given density function and $c_{W,b}(u_i) = \int_W \omega_b(u - u_i) du$ is an edge correction factor that gives higher weight to points near the edge and causes that the estimate is unbiased. Similarly

$$\hat{\rho}_{time}^l(t) = \sum_{i=1}^{N_{R_l}} \frac{\omega'_a(t - t_i^l)}{c_{T,a}(t_i^l)}, \quad t \in T, \quad (4.2)$$

where N_{R_l} is the number of points of the realization, $\omega'_a(t) = \omega'(\frac{t}{a})\frac{1}{a}$ is a probability kernel in \mathbb{R} with bandwidth $a > 0$ where ω' is a given density function and $c_{T,a}(t_i) = \int_T \omega'_a(t - t_i) dt$ is an edge correction factor for time part.

The estimate depends on functions ω, ω' and its bandwidths b, a respectively. However, according to [1], p. 37, the estimate is usually sensitive to the choice of bandwidth, while the choice of the density function is less important. Here we are using the Epanechnikov kernel (see the Section 5.2).

As mentioned higher, we only calculate the estimates in discrete points D of their domain. To determine the best bandwidths, we minimize the sum of square deviations of the estimate from the real intensity function in points of D (see the Section 5.2.1).

The final estimate is

$$\hat{\rho}_{time}(t) = \frac{\sum_{l=1}^n \hat{\rho}_{time}^l(t)}{n}, \quad t \in T, \quad (4.3)$$

$$\hat{\rho}_{space}(u) = \frac{\sum_{l=1}^n \hat{\rho}_{space}^l(u)}{n}, \quad u \in W. \quad (4.4)$$

If we do not suppose space–time separability of ρ , we can do the estimates analogically:

$$\hat{\rho}^l(u, t) = \sum_{i=1}^{N_{R_l}} \frac{\omega''_c((u, t) - (u_i^l, t_i^l))}{c_{W \times T, c}(u_i^l, t_i^l)}, \quad (u, t) \in W \times T, \quad (4.5)$$

where N_{R_l} is the number of points of the realization, $\omega''_c(u, t) = \omega''(\frac{u}{c}, \frac{t}{c})\frac{1}{c^3}$ is a probability kernel in $\mathbb{R}^2 \times \mathbb{R}$ with bandwidth $c > 0$ where ω'' is a given density function and $c_{W \times T, c}(u_i, t_i) = \int_{W \times T} \omega''_c((u, t) - (u_i, t_i)) dudt$ is an edge correction factor. Then the final estimate is

$$\hat{\rho}(u, t) = \frac{\sum_{l=1}^n \hat{\rho}^l(u, t)}{n}, \quad (u, t) \in W \times T. \quad (4.6)$$

4.2 Second order characteristics

The K function is defined in the Definition 10 (see also Definition 9). We would like to estimate the K function of X from simulations in $W \times T$, where X is a space–time point process defined by Model 1, 2 or 3. The estimation is the same for all models. We are also interested in estimation of K_1 and K_2 functions. These functions are possible to define even when the process X is not space–time separable. To judge the space–time separability of X we use the function F (see the Definition 27).

In estimations we need to take care of edge effects for points of X close to the border of the window or for high r and t (compared to the size of the window), where $(r, t) \in W \times T$ are variables of estimated functions. For this reason we use edge correction factors (described lower).

For the reason of a high computational time we estimated these functions only in discrete points of their domain (specified in the Chapter 5). Similarly as in the intensity function estimation, the final estimate is an average from n simulations.

Suppose we have coordinates $(u_i^l, t_i^l) \in X \cap W \times T$ of points of simulations R_l , $l = 1 \dots n$ of the process X in the window $W \times T$. Then an approximately unbiased estimate of function K from simulation R_l is given by (compare with [2], p.476)

$$\widehat{K}^l(r, t) = \frac{1}{|W||T|} \sum_{i \neq j} \frac{I[\|u_i^l - u_j^l\| \leq r, |t_i^l - t_j^l| \leq t]}{\widehat{\rho}(u_i^l, t_i^l) \widehat{\rho}(u_j^l, t_j^l) \omega_1(u_i^l, u_j^l) \omega_2(t_i^l, t_j^l)}, \quad (r, t) \in W \times T, \quad (4.7)$$

where we sum over all pairs of points from X that are not equal (every pair is calculated twice), $\widehat{\rho}(u, t)$ is an estimate for intensity function of X in (u, t) (or we can use the intensity function $\rho(u, t)$ itself), $\omega_1(u_i, u_j)$ is the Ripley's isotropic edge correction factor. This is the reciprocal of the proportion of the circumference of the circle with center u_i and radius $\|u_i - u_j\|$ that lies within W (see [2], p.476), $\omega_2(t_i, t_j)$ is the temporal edge correction factor which is equal to one if both ends of the interval of length $2|t_i - t_j|$ and center t_i lies within T , and $\omega_2(t_i, t_j) = \frac{1}{2}$ otherwise. Then the final estimate is

$$\widehat{K}(r, t) = \frac{\sum_{l=1}^n \widehat{K}^l(r, t)}{n}, \quad (r, t) \in W \times T. \quad (4.8)$$

Similarly, we define $K_1(r)$ and $K_2(t)$ functions:

$$\widehat{K}_1^l(r) = \frac{1}{|W||T|^2} \sum_{i \neq j} \frac{I[\|u_i^l - u_j^l\| \leq r]}{\omega_1(u_i^l, u_j^l) \widehat{\rho}(u_i^l, t_i^l) \widehat{\rho}(u_j^l, t_j^l)}, \quad r \geq 0, \quad (4.9)$$

$$\widehat{K}_2^l(t) = \frac{1}{|W|^2|T|} \sum_{i \neq j} \frac{I[|t_i^l - t_j^l| \leq t]}{\omega_2(t_i^l, t_j^l) \widehat{\rho}(u_i^l, t_i^l) \widehat{\rho}(u_j^l, t_j^l)}, \quad t \geq 0, \quad (4.10)$$

$$\widehat{K}_2(t) = \frac{\sum_{l=1}^n \widehat{K}_2^l(t)}{n}, \quad r \geq 0, \quad (4.11)$$

$$\widehat{K}_1(r) = \frac{\sum_{l=1}^n \widehat{K}_1^l(r)}{n}, \quad r \geq 0. \quad (4.12)$$

Estimate for F is

$$\widehat{F}(r, t) = \frac{\widehat{K}(r, t) - 2\pi r^2 t}{(\widehat{K}_1(r) - \pi r^2)(\widehat{K}_2(t) - 2t)}, \quad \text{where } r, t > 0. \quad (4.13)$$

Chapter 5

Numerical results

We apply the theory from previous chapters to numerically specified parameters and kernel functions. For calculations and graphical output we use software Wolfram Mathematica 9.0. Most of the calculations take a lot of computational time (that depends on the parameters of the model) so there is a limitation of what is possible to calculate. Some calculations depend on statistics with high variance so there is also a limitation of the accuracy of the results. Sometimes doing an average of 100 realizations is not enough to get close to the theoretical value, and doing more would take too much time. However, after some effort we obtained satisfactory results even for ambit models. Some estimates work really well, for example estimate of function F (Figure 5.3(c)) for Model 2 or estimates of K_1 and K_2 functions for all our simulated models.

We are interested in three space–time SNCP models defined in the Section 2.3. Now, we specify the equations and numbers that we use for simulations and estimations.

All models we simulate in the window $W \times T = [0, 1]^2 \times [0, 1]$.

Model 1

We have chosen parameters of Model 1 according to the article [2] to be able to compare the results.

Process Φ_p is a Poisson point process on $\mathbb{R}^3 \times \mathbb{R}_+$ with intensity $\zeta(u, t, r) = \nu \delta_1(r)$, $(u, t, r) \in \mathbb{R}^2 \times \mathbb{R} \times \mathbb{R}_+$, $\nu = 10$, so the point process Φ is a stationary process on \mathbb{R}^3 with intensity $\nu = 10$ and marks are equal to $r = 1$ with probability one.

The kernel k is $k(u, t) = k_1(u)k_2(t)$, $(u, t) \in \mathbb{R}^2 \times \mathbb{R}$ with

$$k_1(u) = \frac{1}{2\pi\sigma^2} \exp\left(-\frac{x^2 + y^2}{2\sigma^2}\right), \quad u = (x, y) \in \mathbb{R}^2, \quad (5.1)$$

$$k_2(t) = \frac{\alpha}{1 - \exp(-\alpha t^*)} \exp(-\alpha t), \quad 0 \leq t \leq t^*, \quad \text{otherwise } k_2(t) = 0, \quad (5.2)$$

where $\sigma = 0.025$, $\alpha = 20$, $t^* = 0.1$.

The function λ is

$$\lambda(u, t) = \frac{20}{(1 - e^{-1})(e - 1)(e^2 - 1)} \exp(-x + y + 2t), \quad (u, t) \in \mathbb{R}^2 \times \mathbb{R}.$$

Note 26. The function λ is not bounded on $\mathbb{R}^2 \times \mathbb{R}$, but it is bounded in the window $W \times T$ where we are observing the process.

The intensity function of X is

$$\rho(u, t) = \nu \lambda(u, t) = \frac{200}{(1 - e^{-1})(e - 1)(e^2 - 1)} \exp(-x + y + 2t), \quad (u, t) \in \mathbb{R}^2 \times \mathbb{R}.$$

The expected number of points of X in the window $W \times T$ is

$$\mathbb{E}X(W \times T) = \int_{W \times T} \rho(u, t) d(u, t) = 100.$$

In the simulation we used a larger window $\bar{W} = [-6\sigma, 1 + 6\sigma] \times [-6\sigma, 1 + 6\sigma] \times [-t^*, 1.0]$ and for bounds for one cluster we used $\Delta_x = \Delta_y = 6\sigma$, $\Delta_{z_d} = t^*$, $\Delta_{z_u} = 0$ (see the Chapter 3 for details of the algorithm). Example of a realization of the process X (blue dots) and the process Φ (red dots) is in the Figure 5.1(a). We notice a higher intensity of points in clusters situated higher and we also notice different volumes of one cluster. Some blue dots come from cluster centers that are not inside $W \times T$ which is in agreement with the algorithm of simulation.

Model 2

Process Φ_p is a Poisson point process on $\mathbb{R}^3 \times \mathbb{R}_+$ with intensity function $\zeta(u, t, r) = \nu \delta_1(r)$, $(u, t, r) \in \mathbb{R}^2 \times \mathbb{R} \times \mathbb{R}_+$, $\nu = 10$, so the point process Φ is a stationary process on \mathbb{R}^3 with intensity $\nu = 10$ and marks are equal to $r = 1$ with probability one.

The kernel k is a density of a uniform distribution on ambit set $A_0(0)$ (see the Definition 28) with parameters $t_1 = 0.1$, $\gamma = \frac{\pi}{6}$. We wanted to make the volume of the clusters in all models similar (even though the kernel k is different).

The function $\lambda(u, t) = 10$ for all $(u, t) \in \mathbb{R}^2 \times \mathbb{R}$ so the intensity function of X is

$$\rho(u, t) = \nu \lambda(u, t) = 100, \quad (u, t) \in \mathbb{R}^2 \times \mathbb{R}.$$

The function λ is constant, but the expected number of points of X in $W \times T$ is the same for Model 1 and 2, $\mathbb{E}X(W \times T) = 100$. Mean number of points in one cluster is

$$\mathbb{E}X_{\xi, \eta, r}(A_\xi(\eta)) = \int_{A_\xi(\eta)} \lambda(u, t) r k(u - \xi, t - \eta) du dt = 10,$$

where r is almost surely one, $(\xi, \eta, r) \in \Phi_p$.

In the simulation we used a larger window $\bar{W} = [-t_1 \operatorname{tg}(\gamma), 1 + t_1 \operatorname{tg}(\gamma)] \times [-t_1 \operatorname{tg}(\gamma), 1 + t_1 \operatorname{tg}(\gamma)] \times [0.0, 1 + t_1]$ and for bounds for one cluster we used $\Delta_x = \Delta_y = t_1 \operatorname{tg}(\gamma)$, $\Delta_{z_d} = 0$, $\Delta_{z_u} = t_1$. Example of a realization of the process X (blue dots) and the process Φ (red dots) is in the Figure 5.1(b). We can see clearly the cone shaped clusters with uniformly distributed points (the projection to two dimensions does not preserve the uniformness).

Model 3

Process Φ_p is a Poisson point process on $\mathbb{R}^3 \times (\epsilon, \infty)$ with intensity function $\zeta(u, t, r) = \nu \iota \frac{1}{r} e^{-\tau r}$, $(u, t, r) \in \mathbb{R}^2 \times \mathbb{R} \times (\epsilon, \infty)$, so the point process Φ is a stationary process on \mathbb{R}^3 with intensity ν and marks have common distribution with density $p(r) = \iota r^{-1} e^{-\tau r}$, $r \in (\epsilon, \infty)$, where $\iota^{-1} = \int_{\epsilon}^{\infty} r^{-1} e^{-\tau r} dr$, $\nu = 10$, $\tau = 0.17$, $\epsilon = 0.01$. These parameters are set to make all three models similar in the mean number of points in one cluster and in the window $W \times T$. Of course the distribution of the number of points in one cluster is different from the Model 2.

In the simulation we used a larger window $\bar{W} = [-t_1 \operatorname{tg}(\gamma), 1 + t_1 \operatorname{tg}(\gamma)] \times [-t_1 \operatorname{tg}(\gamma), 1 + t_1 \operatorname{tg}(\gamma)] \times [0.0, 1 + t_1]$ and for bounds for one cluster we used $\Delta_x = \Delta_y = t_1 \operatorname{tg}(\gamma)$, $\Delta_{z_d} = 0$, $\Delta_{z_u} = t_1$. An example of a realization of the process X (blue dots) and the process Φ (red dots) is in the Figure 5.1(c). Compared to Model 2, there are more clusters with very low number of points and some with very high number of points.

The kernel k is a density of a uniform distribution on ambit set $A_0(0)$ (see the Definition 28) with parameters $t_1 = 0.1$, $\gamma = \frac{\pi}{6}$.

The function $\lambda(u, t) = 10$ for all $(u, t) \in \mathbb{R}^2 \times \mathbb{R}$ so the intensity function of X is

$$\rho(u, t) = \nu \lambda(u, t) \int_{(\epsilon, \infty)} r p(r) dr = \nu \lambda(u, t) \iota \frac{e^{-\tau \epsilon}}{\tau} = 101.22, \quad (u, t) \in \mathbb{R}^2 \times \mathbb{R}$$

The expected number of points of X in $W \times T$ is $\mathbb{E}X(W \times T) = 101.22$ and expected number of points in one cluster is

$$\begin{aligned} \mathbb{E}\mathbb{E}[X_{\xi, \eta, r}(A_{\xi}(\eta)) | r = \hat{r}] &= \mathbb{E} \int_{A_{\xi}(\eta)} \lambda(u, t) \hat{r} k(u - \xi, t - \eta) du dt \\ &= 10 \mathbb{E} \hat{r} = 10 \int_{\epsilon}^{\infty} r p(r) dr = 10.122. \end{aligned} \tag{5.3}$$

5.1 Theoretical characteristics

For our models it is possible to derive some theoretical characteristics explicitly. We have already calculated the intensity function for all three models. In this chapter we want to have a closer look on F , K and g functions.

5.1.1 Calculation of function F for Model 1

We can derive formula for F as follows.

Suppose that we are in the situation of Model 1. Then $k(u, t) = k_1(u)k_2(t)$ and g function is of the form

$$g(u, t) = 1 + \frac{\int_{\mathbb{R}} \int_{\mathbb{R}^2} k(x - u, y - t)k(x, y)dxdy}{\nu} = 1 + \frac{k * \tilde{k}(u, t)}{\nu}, \quad (5.4)$$

$(u, t) \in \mathbb{R}^2 \times \mathbb{R}$, $\tilde{k}(-x, -y) = k(x, y)$ and $k * \tilde{k}(u, t)$ is a convolution of functions k and \tilde{k} . Then g_1 and g_2 functions defined by (2.12) and (2.13) are

$$\begin{aligned} g_1(u) &= \frac{1}{|T|^2} \int_T \int_T g(u, s - t)dsdt = \frac{1}{|T|^2} \int_T \int_T \left(1 + \frac{k * \tilde{k}(u, s - t)}{\nu} \right) dsdt \\ &= 1 + \frac{k_1 * \tilde{k}_1(u)}{\nu_1} \end{aligned} \quad (5.5)$$

and

$$\begin{aligned} g_2(t) &= \frac{1}{|W|^2} \int_W \int_W g(u - v, t)dudv = \frac{1}{|W|^2} \int_W \int_W \left(1 + \frac{k * \tilde{k}(u - v, t)}{\nu} \right) dudv \\ &= 1 + \frac{k_2 * \tilde{k}_2(t)}{\nu_2}, \end{aligned} \quad (5.6)$$

where

$$\nu_1 = |T|^2 \nu \left(\int_T \int_T k_2 * \tilde{k}_2(s - t)dsdt \right)^{-1}$$

and

$$\nu_2 = |W|^2 \nu \left(\int_W \int_W k_1 * \tilde{k}_1(u - v)dudv \right)^{-1}.$$

Now we can see that

$$\nu (g(u, t) - 1) = \nu_1 \nu_2 (g_1(u) - 1) (g_2(t) - 1)$$

and integrating with respect to u and t for $\|u\| \leq r$ and $|t| \leq s$ (see (2.14),(2.15)) we obtain

$$\nu (K(r, s) - 1) = \nu_1 \nu_2 (K_1(r) - 1) (K_2(s) - 1), \quad r, t > 0.$$

It is clear, that F from the Definition 27 is constant (see [2], p. 482), and

$$F(r, t) = \frac{\nu_1 \nu_2}{\nu}, \quad r, t > 0.$$

Note 27. It is also possible to derive a more general form for F for any space–time SNCP X with a space–time separable kernel k . By the same method we would obtain

$$F(r, t) = \frac{\nu_1 \nu_2}{\nu} \frac{\left(\int_{\mathbb{R}_+} rp(r)dr \right)^2}{\int_{\mathbb{R}_+} r^2 p(r)dr}, \quad r, t > 0.$$

Now we can continue with the calculation in the situation of Model 1:

$$F(r, t) = \nu \left(\int_W \int_W k_1 * \tilde{k}_1(u - v) dudv \right)^{-1} \left(\int_T \int_T k_2 * \tilde{k}_2(s - t) dsdt \right)^{-1} \quad (5.7)$$

$$= \nu P_1^{-1} P_2^{-1},$$

where $u, v \in \mathbb{R}^2$, $s, t \in \mathbb{R}$ and $\tilde{k}_1(-u) = k_1(u)$ and $\tilde{k}_2(-t) = k_2(t)$, by P_1, P_2 we denote first part, second part respectively.

The first convolution is

$$k_1 * \tilde{k}_1(u - v) = \int_{\mathbb{R}^2} k_1(c) \tilde{k}_1(u - v - c) dc = \int_{\mathbb{R}^2} k_1(c) k_1(c + v - u) dc, \quad \text{where } u, v \in \mathbb{R}^2.$$

Then using (5.1) and $c = (c_1, c_2)$, $u = (u_1, u_2)$, $v = (v_1, v_2)$, we have:

$$\int_{\mathbb{R}} \int_{\mathbb{R}} \left(\frac{1}{2\pi\sigma^2} \right)^2 e^{-\frac{c_1^2 + c_2^2}{2\sigma^2}} e^{-\frac{(c_1 + v_1 - u_1)^2 + (c_2 + v_2 - u_2)^2}{2\sigma^2}} dc_1 dc_2$$

and separating c_1 and c_2 from the rest we get

$$\left(\frac{1}{2\pi\sigma^2} \right)^2 e^{-\frac{(v_1 - u_1)^2}{4\sigma^2}} e^{-\frac{(v_2 - u_2)^2}{4\sigma^2}} \int_{\mathbb{R}} \int_{\mathbb{R}} e^{-\frac{(c_1 + \frac{(v_1 - u_1)^2}{2})^2 + (c_2 + \frac{(v_2 - u_2)^2}{2})^2}{2\sigma^2}} dc_1 dc_2. \quad (5.8)$$

After this we need the second convolution

$$k_2 * \tilde{k}_2(s - t) = \int_{\mathbb{R}} k_2(c) \tilde{k}_2(s - t - c) dc = \int_{\mathbb{R}} k_2(c) k_2(t + c - s) dc,$$

$s, t \in \mathbb{R}$. Now we denote $\Gamma = \frac{\alpha}{1 - e^{-\alpha t^*}}$ and set $0 \leq c \leq t^*$, $-t^* \leq t - s \leq t^*$, because otherwise the convolution is equal to zero. At first, for $0 \leq t - s \leq t^*$ we have (using (5.2))

$$\int_0^{t^* + s - t} \Gamma e^{-\alpha c} \Gamma e^{-\alpha(t + c - s)} dc = \Gamma^2 e^{-\alpha(t - s)} \int_0^{t^* + s - t} e^{-2\alpha c} dc$$

which we easily adjust to

$$\frac{\Gamma^2}{2\alpha} e^{-\alpha(t - s)} (1 - e^{-2\alpha(t^* + s - t)}), \quad \text{where } 0 \leq t - s \leq t^*.$$

To integrate this convolution, we only need to divide the integral in two parts:

$$\begin{aligned} & \frac{\Gamma^2}{2\alpha} \int_T \int_T I_{[0 \leq t - s \leq t^*]} e^{-\alpha(t - s)} (1 - e^{-2\alpha(t^* + s - t)}) dsdt \\ &= \frac{\Gamma^2}{2\alpha} \left(\int_0^{t^*} \int_0^t e^{-\alpha(t - s)} (1 - e^{-2\alpha(t^* + s - t)}) dsdt \right. \\ & \quad \left. + \int_{t^*}^1 \int_{t - t^*}^t e^{-\alpha(t - s)} (1 - e^{-2\alpha(t^* + s - t)}) dsdt \right) \\ &= \frac{1}{2(1 - e^{-\alpha t^*})^2} \left(1 - 2e^{-\alpha t^*} (1 - t^*) + e^{-2\alpha t^*} + \frac{e^{-2\alpha t^*} - 1}{\alpha} \right) = \frac{P_2}{2}. \end{aligned} \quad (5.9)$$

The last equation (P_2 is defined in (5.7)) we can verify by analogical calculation for $-t^* \leq t - s \leq 0$ or by noticing that the convolution has the same value for $t - s$ positive and $t - s$ negative.

Now we can obtain numerical results. The integral in (5.8) is equal to $\pi\sigma^2$, because we are integrating product of two distribution functions (without the constant part) of normal distribution with variance $\frac{\sigma^2}{2}$ over the whole real line. Using mathematical software, we calculate that

$$P_1 = \int_W \int_W \frac{1}{4\pi\sigma^2} e^{-\frac{(v_1-u_1)^2}{4\sigma^2}} e^{-\frac{(v_2-u_2)^2}{4\sigma^2}} dudv = 0.944377,$$

where we used $\sigma = 0.025$, $W = [0, 1]$ according to the definition of Model 1.

From (5.9) we calculate that

$$P_2 = 0.970551,$$

using $t^* = 0.1$, $\alpha = 20$, $T = [0, 1]$.

Finally we put these results together

$$F(r, t) = \nu P_1^{-1} P_2^{-1} = 10 \frac{1}{0.944377} \frac{1}{0.970551} = 10.9103.$$

5.1.2 Calculation of g function for Model 1

It is possible to express the pair correlation function g for Model 1 in the following form (in (2.26) we set $(v, s) = (0, 0)$):

$$g(u, t) = 1 + \frac{1}{\nu} \int_{\mathbb{R}} \int_{\mathbb{R}^2} k(\tilde{x} - u, z - t) k(\tilde{x}, z) d\tilde{x} dz. \quad (5.10)$$

Since $k(u, t) = k_1(u)k_2(t)$, $(u, t) \in \mathbb{R}^2 \times \mathbb{R}$, the integral is

$$\int_{\mathbb{R}} \int_{\mathbb{R}^2} k(\tilde{x} - u, z - t) k(\tilde{x}, z) d\tilde{x} dz = \int_{\mathbb{R}^2} k_1(\tilde{x} - u) k_1(\tilde{x}) d\tilde{x} \int_{\mathbb{R}} k_2(z - t) k_2(z) dz.$$

Setting $\tilde{x} = (x, y)$, $u = (x_0, y_0)$ we can calculate the first part:

$$\begin{aligned} \int_{\mathbb{R}^2} k_1(\tilde{x} - u) k_1(\tilde{x}) d\tilde{x} &= \int_{\mathbb{R}} \int_{\mathbb{R}} \left(\frac{1}{2\pi\sigma^2} \right)^2 e^{-\frac{(x-x_0)^2 + (y-y_0)^2}{2\sigma^2}} e^{-\frac{x^2 + y^2}{2\sigma^2}} dx dy \\ &= \int_{\mathbb{R}} \frac{1}{2\pi\sigma^2} e^{-\frac{(x-\frac{x_0}{2})^2 + (\frac{x_0}{2})^2}{\sigma^2}} \int_{\mathbb{R}} \frac{1}{2\pi\sigma^2} e^{-\frac{(y-\frac{y_0}{2})^2 + (\frac{y_0}{2})^2}{\sigma^2}} \\ &= \frac{1}{\sqrt{4\pi\sigma^2}} e^{-\left(\frac{x_0}{2\sigma^2}\right)^2} \frac{1}{\sqrt{4\pi\sigma^2}} e^{-\left(\frac{y_0}{2\sigma^2}\right)^2}, \end{aligned}$$

where we used

$$\int_{\mathbb{R}} \frac{\sqrt{2}}{\sqrt{2\pi\sigma^2}} e^{-\frac{(x-\frac{x_0}{2})^2}{\sigma^2}} dx = 1$$

for the first integral and

$$\int_{\mathbb{R}} \frac{\sqrt{2}}{\sqrt{2\pi\sigma^2}} e^{-\frac{(y-\frac{y_0}{2})^2}{\sigma^2}} dy = 1$$

for the second integral.

In the second part, we first calculate the integral for t non-negative.

$$\begin{aligned} \int_{\mathbb{R}} k_2(z-t)k_2(z)dz &= \int_{\mathbb{R}} \left(\frac{\alpha}{1-e^{\alpha t^*}}\right)^2 e^{-\alpha(z-t)}e^{\alpha z} \mathbf{I}[0 \leq z-t \leq t^*] \mathbf{I}[0 \leq z \leq t^*] dz \\ &= \left(\frac{\alpha}{1-e^{\alpha t^*}}\right)^2 e^{\alpha t} \int_t^{t^*} e^{-2\alpha z} dz \\ &= \frac{\alpha (e^{-\alpha t} - e^{\alpha(t-2t^*)})}{2(1-e^{-\alpha t^*})^2}, \quad 0 \leq t \leq t^*. \end{aligned} \tag{5.11}$$

Using analogical calculation (or also directly) we can see that the integral has the same value for t negative. So the second part is equal to

$$\frac{\alpha (e^{-\alpha|t|} - e^{\alpha(|t|-2t^*)})}{2(1-e^{-\alpha t^*})^2}, \quad 0 \leq |t| \leq t^*.$$

Putting (5.10) and these two parts together we obtain ($u = (x_0, y_0)$):

$$g(u, t) = 1 + \frac{\alpha e^{-\frac{x_0^2+y_0^2}{4\sigma^2}} (e^{-\alpha|t|} - e^{\alpha(|t|-2t^*)})}{8\nu\pi\sigma^2 (1-e^{-\alpha t^*})^2} \mathbf{I}[0 \leq |t| \leq t^*], \tag{5.12}$$

$(u, t) \in \mathbb{R}^2 \times \mathbb{R}$.

Since we have

$$g(x, y, t) = g(\sqrt{x^2 + y^2}, 0, t) = \tilde{g}(r, t), \quad r, t \geq 0,$$

where r is the Euclidean distance from the origin, we can graphically visualize values of g function using plot of \tilde{g} function – see Figure 5.6(a).

Using (5.12) and (2.14), (2.15), (2.11), we can calculate theoretical K_1 , K_2 functions (see Figure 5.2) and K function (see Figure 5.5(a)) for Model 1:

$$K_1(r) = \frac{1}{|T|^2} \int_{\|u\| \leq r} \int_T \int_T \left(1 + \frac{\alpha e^{-\frac{x_0^2+y_0^2}{4\sigma^2}} (e^{-\alpha|s-t|} - e^{\alpha(|s-t|-2t^*)})}{8\nu\pi\sigma^2 (1-e^{-\alpha t^*})^2} \right) \mathbf{I}[0 \leq |s-t| \leq t^*] ds dt du, \tag{5.13}$$

$$K_2(t) = \frac{1}{|W|^2} \int_{-t}^t \int_W \int_W \left(1 + \frac{\alpha e^{-\frac{(x_0-x_1)^2+(y_0-y_1)^2}{4\sigma^2}} (e^{-\alpha|s|} - e^{\alpha(|s|-2t^*)})}{8\nu\pi\sigma^2 (1-e^{-\alpha t^*})^2} \right) \mathbf{I}[0 \leq |s| \leq t^*] dv du ds, \tag{5.14}$$

$$K(r, t) = \int_{\|u\| \leq r} \int_{-t}^t \left(1 + \frac{\alpha e^{-\frac{(x_0)^2 + (y_0)^2}{4\sigma^2}} (e^{-\alpha|s|} - e^{\alpha(|s| - 2t^*)})}{8\nu\pi\sigma^2 (1 - e^{-\alpha t^*})^2} \right) I[0 \leq |s| \leq t^*] ds du$$

where $u = (x_0, y_0) \in \mathbb{R}^2$, $v = (x_1, y_1) \in \mathbb{R}^2$, $t \geq 0$.

5.1.3 Calculation of g function for Model 2, 3

We already know from the Chapter 2, that the pair correlation function g for Model 2 is

$$g(u, t) = 1 + \frac{|A_u(t) \cap A_0(0)|}{\nu |A_0(0)|^2} = 1 + c_1 |A_u(t) \cap A_0(0)|$$

and for Model 3

$$g(u, t) = 1 + \frac{1 + \epsilon\tau}{\nu e^{-\epsilon\tau}} \frac{|A_u(t) \cap A_0(0)|}{|A_0(0)|^2} = 1 + c_2 |A_u(t) \cap A_0(0)|,$$

where $(u, t) \in \mathbb{R}^2 \times \mathbb{R}$. We can evaluate constants c_1 and c_2 easily, all parameters are defined higher (volume of the cone is calculated from angle γ and its height t_1) and numerical results are $c_1 = 820702$ and $c_2 = 4776000$. For the volume of the intersection of two cones $A_0(0)$ and $A_{(x,y)}(z)$ with the same t_1 and γ we derived an explicit formula

$$\text{Intersection}(x, y, z) = |A_{(x,y)}(z) \cap A_0(0)| \quad (5.15)$$

that the reader can find at the end of this chapter. This formula is a result from the mathematical software, but the calculation was not straightforward. We had to divide the problem in more simple parts, integrate these parts as far as it was possible, then use the software to finish the integration and then put these parts together. The explicit formula (5.15) is necessary for calculating the F function, because by numerical integration alone it is not possible to obtain values of F function (see the Definition 27) with satisfactory accuracy (which is necessary for recognizing its shape) due to multiple integration.

From the isotropy in spatial coordinates of Models 2, 3 we can visualize the g function as a function of time and the distance from origin in the spatial coordinate setting $\tilde{g}(r, t) = g(\sqrt{x^2 + y^2}, 0, t) = g(x, y, t)$, where $r = \sqrt{x^2 + y^2}$ (see Figures 5.6(b) and 5.6(c)).

Theoretical values of K_1 , K_2 , K , F functions we calculate only numerically using explicit formula (5.15). There are still many multiple integrals, but the accuracy is good. See Figures 5.3 and 5.4.

$$K_1(r) = \int_{\|u\| \leq r} \int_T \int_T (1 + \phi \text{Intersection}(u, s - t)) ds dt du,$$

$$K_2(t) = \int_{-t}^t \int_W \int_W (1 + \phi \text{Intersection}(u - v, s)) dv du ds$$

$$K(r, t) = \int_{\|u\| \leq r} \int_{-t}^t (1 + \phi \text{Intersection}(u, s)) ds du$$

$$F(r, t) = \frac{K(r, t) - 2\pi r^2 t}{(K_1(r) - \pi r^2)(K_2(t) - 2t)},$$

where $u = (x, y) \in \mathbb{R}^2$, $t \geq 0$ and $\phi = c_1$ for Model 2, or $\phi = c_2$ for Model 3.

5.2 Estimation results

5.2.1 Intensity estimate

The Epanechnikov kernel used for intensity estimation (see the Section 4.1) has following forms (depending on the dimension):

$$\omega'(t) = \frac{3}{4}(1 - t^2) I[-1 \leq t \leq 1], \quad t \in \mathbb{R}$$

for time part estimation,

$$\omega(u) = \frac{2}{\pi}(1 - x^2 - y^2) I[x^2 + y^2 \leq 1], \quad u = (x, y) \in \mathbb{R}^2$$

for space part and

$$\omega''(u, t) = \frac{15}{8\pi}(1 - x^2 - y^2 - t^2) I[x^2 + y^2 + t^2 \leq 1], \quad u = (x, y) \in \mathbb{R}^2, t \in \mathbb{R}$$

for non-separable space and time.

To determine the best bandwidths we used the following three methods. Firstly we minimized the sum of square deviations of the estimate (from 100 simulations) from the real intensity function in a certain number of equidistantly selected points of their domain. That is, to determine a we minimized

$$\sum_{i=1}^{10} \left(\widehat{\rho}_{time}^a \left(\frac{i}{10} \right) - \rho_{time} \left(\frac{i}{10} \right) \right)^2 \quad (5.16)$$

over $a \in (0, 1)$ where $\widehat{\rho}_{time}^a$ is an average of the kernel estimates of ρ_{time} with bandwidth a , to determine b we minimized

$$\sum_{i,j=1}^{10} \left(\widehat{\rho}_{space}^b \left(\frac{i}{10}, \frac{j}{10} \right) - \rho_{space} \left(\frac{i}{10}, \frac{j}{10} \right) \right)^2 \quad (5.17)$$

over $b \in (0, 1)$ where $\widehat{\rho}_{space}^b$ is an average of the kernel estimate of ρ_{space} with bandwidth b , to determine c we minimized

$$\sum_{i,j,k=1}^{10} \left(\widehat{\rho}^c \left(\frac{i}{10}, \frac{j}{10}, \frac{k}{10} \right) - \rho \left(\frac{i}{10}, \frac{j}{10}, \frac{k}{10} \right) \right)^2 \quad (5.18)$$

over $c \in (0, 1)$ where $\widehat{\rho}^c$ is an average of the kernel estimate of ρ with bandwidth c (see the Table 5.2.1 for results).

Table 5.1: Sum of square errors for intensity function estimate from 100 simulations.

bandwidth	Model 1 – time	Model 1 – space	Model 2	Model 3
0.05	6563	142813	1.2×10^7	3.9×10^7
0.10	12114	51912	2.8×10^6	1.5×10^7
0.15	8051	55573	1.3×10^6	5.4×10^6
0.20	7518	59545	0.8×10^6	2.4×10^6
0.25	8556	42159	0.5×10^6	1.7×10^6
0.30	14242	46453	0.5×10^6	1.0×10^6
0.35	12397	58350	0.6×10^6	0.7×10^6
0.40	15571	54986	0.4×10^6	1.1×10^6

Secondly, because the estimate is a random variable we also tried other bandwidths and checked the result visually. Thirdly, the minimization depends on the real intensity function that we do not know from simulations but from theory. That is why we also adjusted the estimated bandwidth (if it was too high) comparing to the size of the window.

Approximately best values (in the situation of Model 1) are $a = 0.05$ and $b = 0.2$ and $c = 0.4$ for Models 2 and 3 respectively.

Estimated intensity for Model 1 is shown in Figures 5.2(c) (time part) and 5.2(d) (space part). We can see that the estimate fits the real functions quite well.

Note 28. We found out that our estimates for a and b differ from those in [2], p.484. They suggest values $b = 0.067$ and $a = 0.6$ (see [2], p.15). But we find our estimates more suitable and as is shown further, they work well in the estimation of F and K functions.

5.2.2 Estimation of K and F function

We did the estimation of K function in discrete points $(r, t) = (r_i, t_i) \in [0, 1] \times [0, 1]$ where $r_i = \frac{i}{100}$, $t_i = \frac{i}{100}$, $i = 1 \dots 100$. Function $K_1(r)$ was estimated for $r = r_i = \frac{i}{100}$, $i = 1, \dots 100$ and $K_2(t)$ was estimated for $t = t_i = \frac{i}{100}$, $i = 1, \dots 100$. We are using (4.8), (4.11) and (4.12). Number of simulations $n = 100$ was used for estimation of these functions.

Calculation of time edge correction $\omega_2(t_i, t_j)$ is quite straightforward. On the other hand, to calculate space edge correction $\omega_1(u_i, u_j)$ for two different points u_i, u_j of the process X we need to use formula ArcLength (5.19), where t is the Euclidean distance of u_i and u_j , $t \in (0, 1]$ and $(x, y) = u_i \in [0, 1] \times [0, 1]$ are the spatial coordinates of the first point. Then

$$\omega_1(u_i, u_j) = \text{ArcLength}(x, y, \|u_i - u_j\|),$$

$u_i \neq u_j$. After considering all possible cases we get formula

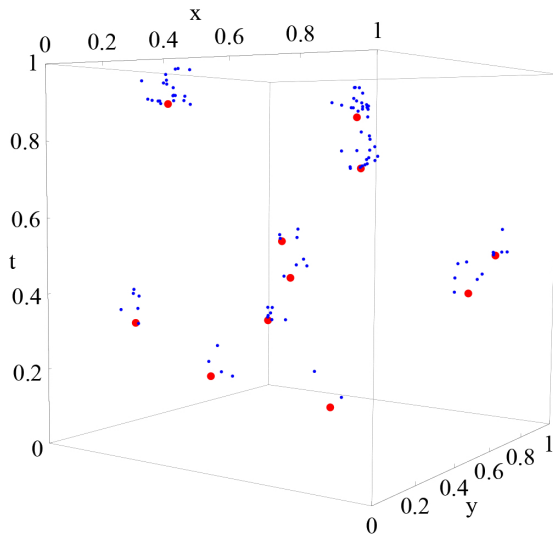
$$\begin{aligned}
\text{ArcLength}(x, y, t) = & \\
& \frac{1}{2\pi} \left(\mathbb{I}[y \leq 1 - t] \left(\arcsin \left(\min\left(\frac{x}{t}, 1\right)\right) + \arcsin \left(\min\left(\frac{1-x}{t}, 1\right)\right) \right) \right) \\
& + \mathbb{I}[t \leq y] \left(\arcsin \left(\min\left(\frac{x}{t}, 1\right)\right) + \arcsin \left(\min\left(\frac{1-x}{t}, 1\right)\right) \right) \\
& + \mathbb{I}[x^2 + (1 - y^2) \geq t^2, y > 1 - t, x < t] \left(\frac{\pi}{2} - \arccos \left(\frac{x}{t} \right) - \arccos \left(\frac{1-y}{t} \right) \right) \\
& + \mathbb{I}[x^2 + y^2 \geq t^2, y < t, x < t] \left(\frac{\pi}{2} - \arccos \left(\frac{x}{t} \right) - \arccos \left(\frac{y}{t} \right) \right) \\
& + \mathbb{I}[(1-x)^2 + (1-y)^2 \geq t^2, y > 1-t, x > 1-t] \\
& \quad \left(\frac{\pi}{2} - \arccos \left(\frac{1-x}{t} \right) - \arccos \left(\frac{1-y}{t} \right) \right) \\
& + \mathbb{I}[(1-x)^2 + y^2 \geq t^2, y < t, x > 1-t] \left(\frac{\pi}{2} - \arccos \left(\frac{1-x}{t} \right) - \arccos \left(\frac{y}{t} \right) \right) \\
& + \mathbb{I}[y > 1-t, x > t] \arcsin \left(\frac{1-y}{t} \right) + \mathbb{I}[y > 1-t, x < 1-t] \arcsin \left(\frac{1-y}{t} \right) \\
& + \mathbb{I}[y < t, x > t] \arcsin \left(\frac{y}{t} \right) + \mathbb{I}[y < t, x < 1-t] \arcsin \left(\frac{y}{t} \right) \Big).
\end{aligned} \tag{5.19}$$

Estimated K_1 and K_2 functions using either the real intensity function or estimated intensity functions together with corresponding theoretical functions are in Figures 5.2(e), 5.2(f) for Model 1, 5.3(a), 5.3(b) for Model 2 and 5.4(a), 5.4(b) for Model 3. We can notice that all curves fit the theoretical ones very well, the estimate using estimated intensity function is naturally a little bit worse. All curves are above theoretical K_1 resp. K_2 functions for Poisson process (blue line).

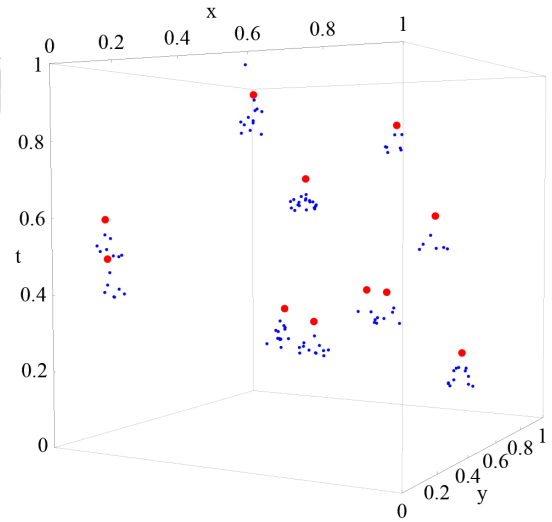
Estimated and theoretical K function for all three models is in the Figure 5.5. We show the result of estimation using the real intensity function as well as using the estimated intensity function. The result of estimation is good, we can see that the estimated functions are close to their theoretical equivalent for all three models.

We know from the Section 5.1.1 that F function for Model 1 which has space-time separable distribution of points in one cluster is constant and $F(r, t) \doteq 10.9$, $r, t > 0$. Moreover we have shown in the calculation that when the kernel k is space-time separable then the function F is constant for any space-time SNCP. It means that having some simulated data, we can use the Formula (4.13) to check the separability of k of the theoretical model. Under the separability hypothesis $k(u, t) = k_1(u)k_2(t)$, $(u, t) \in [0, 1]^2$ we can expect (4.13) to be approximately constant. On the other hand, for Model 2 and 3 the estimated F function should not be constant (see the theoretical F function for Model 2 in Figure 5.3(e), and for Model 3 in Figure 5.4(e)).

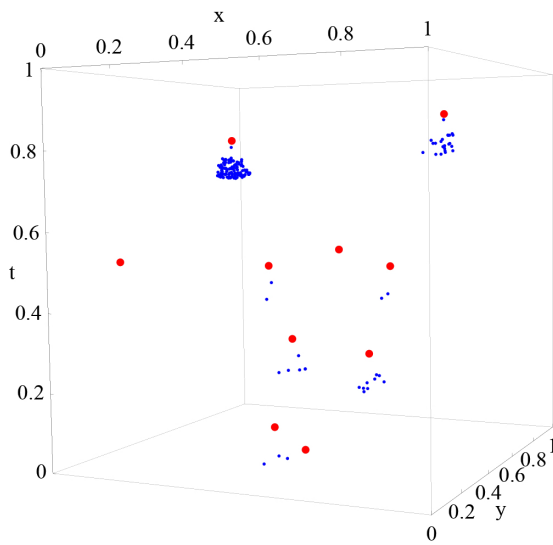
Estimate \widehat{F} (4.13) is a ratio estimator and has higher variance than estimates \widehat{K} , \widehat{K}_1 , \widehat{K}_2 because it combines deviations of these estimates from their theoretical equivalents. Because of this, we calculated estimates of F from $n = 1000$ simulations. The result for Model 2 (see Figure 5.3(c)), using the theoretical intensity function is very precise and the shape is almost the same as that of the theoretical F function for this model and shows non-separability of the kernel k . The estimate using the estimated intensity function is worse (see Figure 5.3(d)). For Model 3 estimates of \widehat{F} using $\widehat{\rho}$ and ρ (see Figures 5.4(c), 5.4(d)) are both close to the theoretical F function. The estimate for Model 1 is close to the real value of F , but it is constant only approximately. Probably, this is due to higher variance of \widehat{F} for Model 1 than for Model 2, 3.



(a) Model 1



(b) Model 2



(c) Model 3

Figure 5.1: Realization of a point process from Model 1, Model 2 and Model 3. The vertical axis is temporal, the other two axis are spatial.

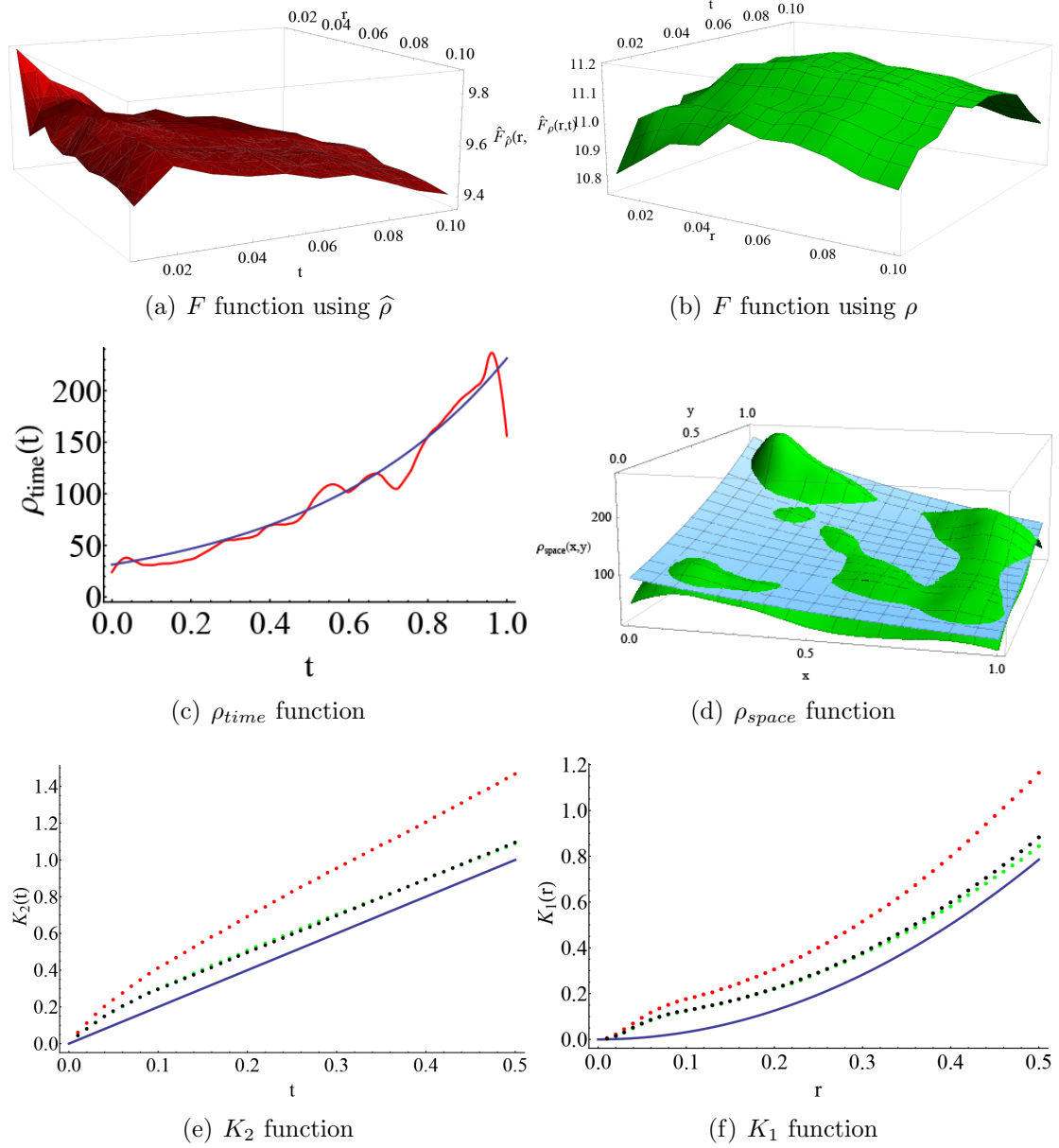


Figure 5.2: Model 1. First row: estimates of F function. Second row: (c) blue line is the real ρ_{time} function, red line is an estimate, (d) blue surface is the real ρ_{space} function, green surface is an estimate. Third row: red dots are estimates of K_1 (f) and K_2 (e) functions using estimate of intensity function, green dots are estimates using the theoretical intensity function, blue line is function $2t$ (e) and πr^2 (f).

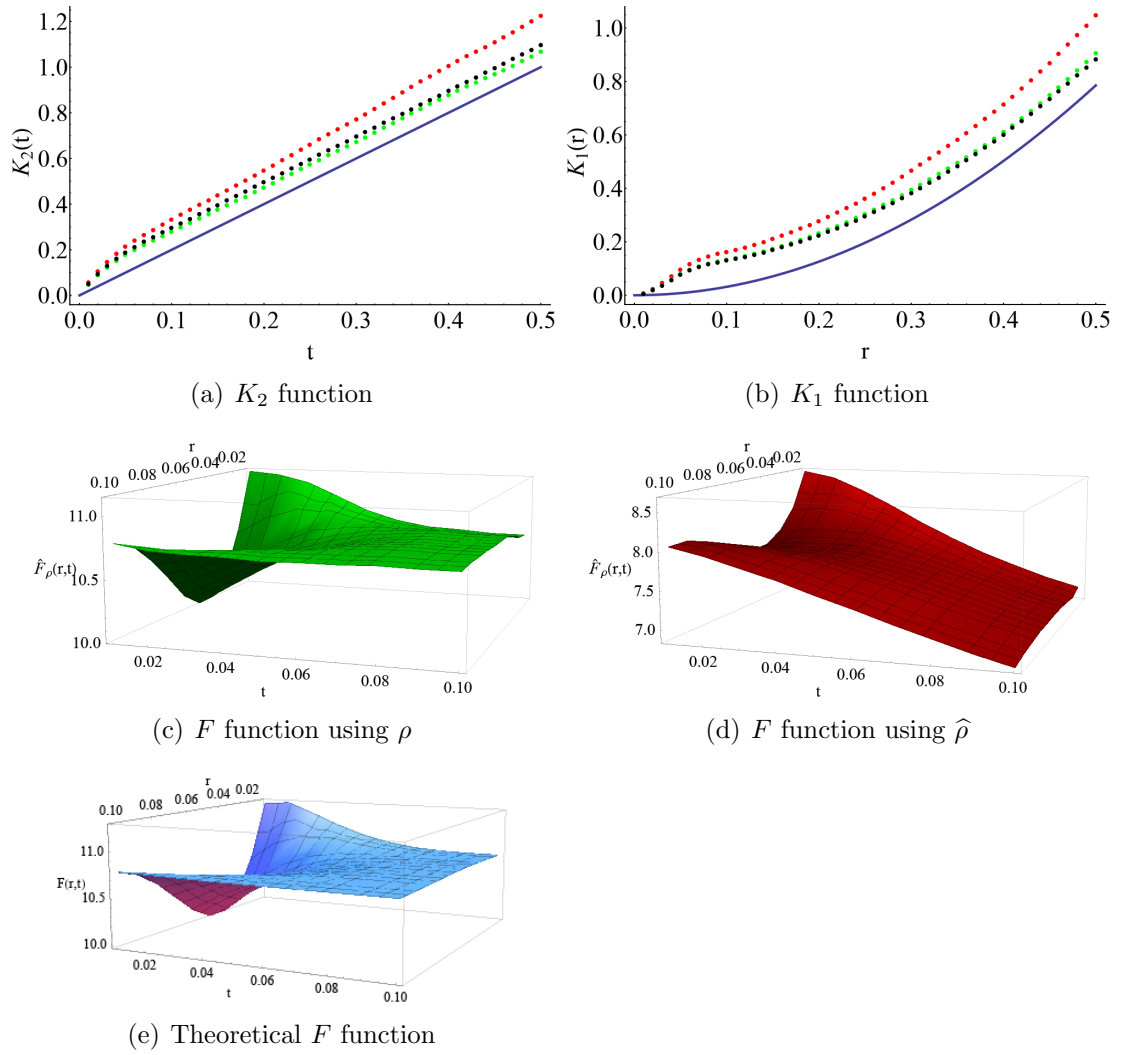


Figure 5.3: Model 2. First row: black dots are real K_2 (a) and K_1 (b) functions, green dots are estimates of K_2 (a) and K_1 (b) functions, red dots are estimates using estimate of intensity function, blue line is function $2t$ (a) and πr^2 (b). Second row: (c) estimate of F function using real intensity function, (d) estimate of F function using estimate of intensity function. Third row: theoretical F function.

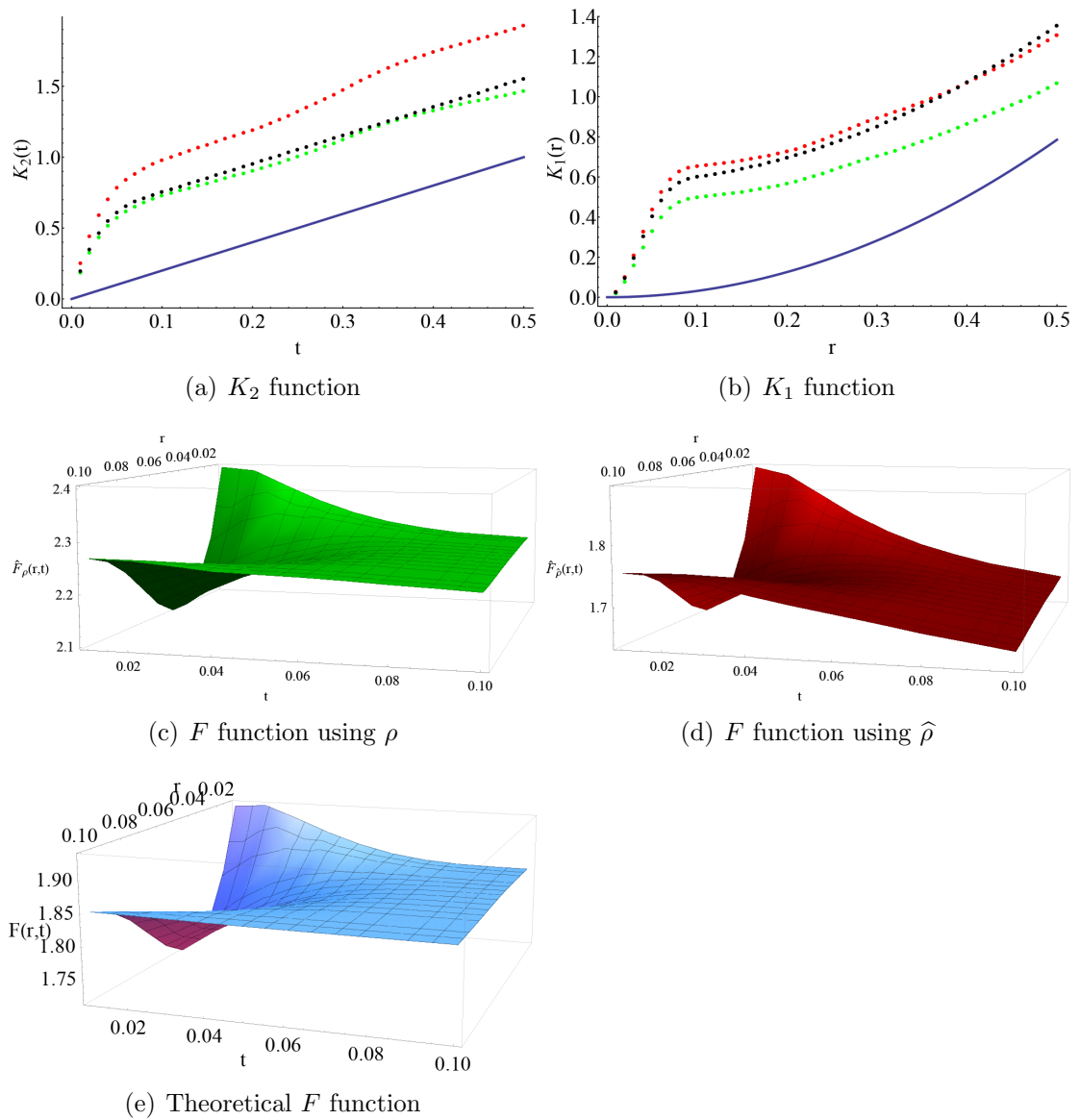


Figure 5.4: Model 3. First row: black dots are real K_2 (a) and K_1 (b) functions, green dots are estimates of K_2 (a) and K_1 (b) functions, red dots are estimates using estimate of intensity function, blue line is function $2t$ (a) and πr^2 (b). Second row: (c) estimate of F function using real intensity function, (d) estimate of F function using estimate of intensity function. Third row: theoretical F function.

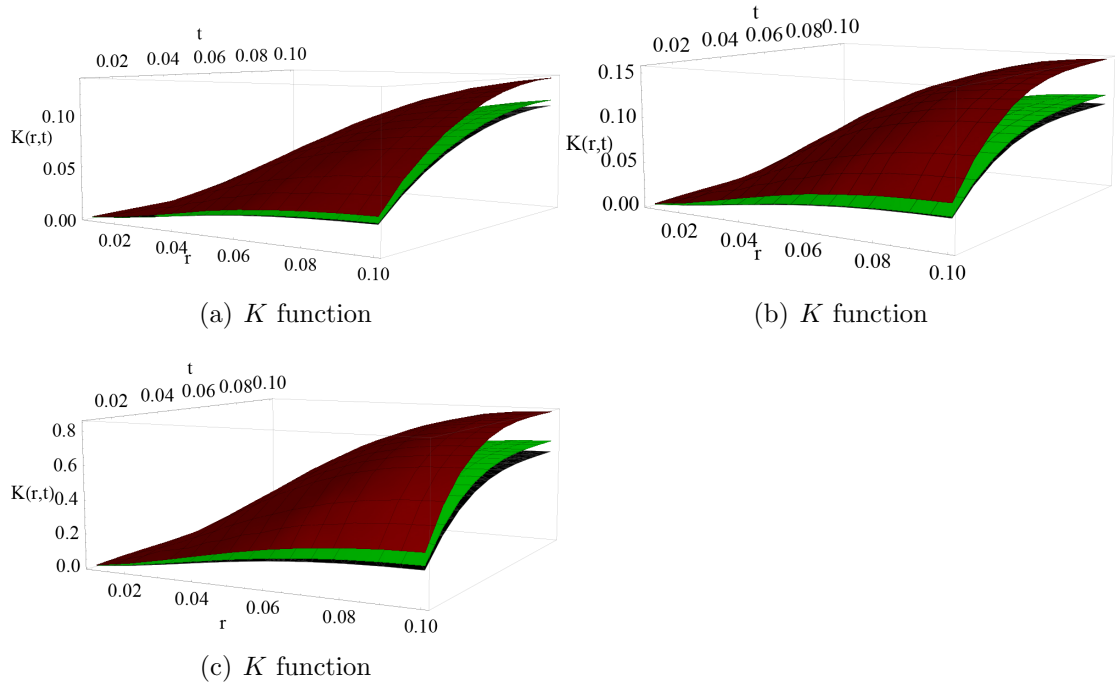


Figure 5.5: K function for Model 1 (a), for Model 2 (b) and for Model 3 (c). For each figure, there are three surfaces. Black surface is the theoretical K function (for the corresponding model with numerically specified parameters), green surface is the estimated K function using the theoretical intensity function and red surface is the estimated K function using the estimated intensity function.

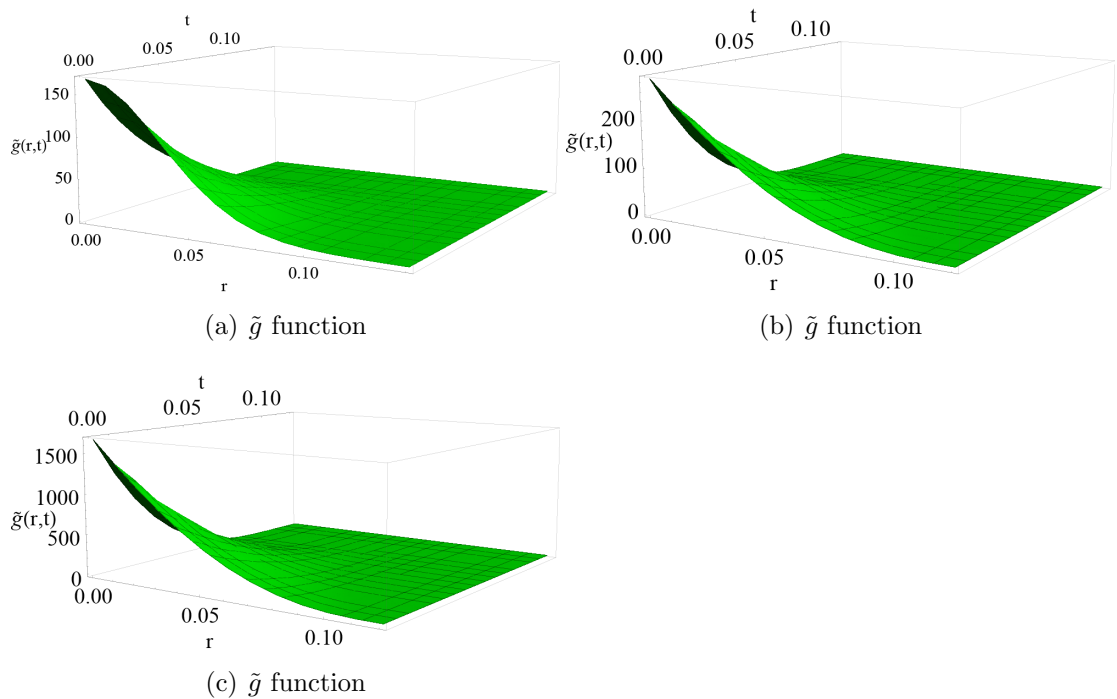


Figure 5.6: Pair correlation functions for Model 1 (a) for Model 2 (b) and for Model 3 (c) (with numerically specified parameters) as a function of time and the distance from the origin in the spatial coordinate. Values in point $(0,0)$: (a) $\tilde{g}(0,0) \doteq 168$, (b) $\tilde{g}(0,0) \doteq 287$, (c) $\tilde{g}(0,0) \doteq 1669$.

$$\begin{aligned}
\text{IntersectionY}(x, z) = & \text{I}[0 \leq z \leq t_1, 0 \leq x \leq (t_1 - z) \text{tg}(\gamma)] \frac{1}{3} \pi z (\text{tg}(\gamma) z)^2 \\
& + \text{I}[0 \leq z \leq t_1, (t_1 - z) \text{tg}(\gamma) < x < (t_1 + z) \text{tg}(\gamma)] \left[-8 \text{tg}(\gamma) (x + \text{tg}(\gamma)(t_1 - z)) \right. \\
& (t_1 + z) (x + \text{tg}(\gamma)(-t_1 + z)) \sqrt{(-x + \text{tg}(\gamma)(t_1 + z)) (x + \text{tg}(\gamma)(t_1 + z))} \\
& \left. + \pi \left(8 \text{tg}^3(\gamma) \sqrt{x^2 - \text{tg}^2(\gamma)(t_1 - z)^2} (t_1^3 + z^3) \right) \right. \\
& - 16 \text{tg}^3(\gamma) t_1^3 \sqrt{x^2 - \text{tg}^2(\gamma)(t_1 - z)^2} \operatorname{arccsc} \left(\frac{2 \text{tg}(\gamma) t_1 x}{x^2 + \text{tg}^2(\gamma)(t_1 - z)(t_1 + z)} \right) \\
& - 16 \text{tg}^3(\gamma) \sqrt{x^2 - \text{tg}^2(\gamma)(t_1 - z)^2} z^3 \operatorname{arccsc} \left(\frac{2 \text{tg}(\gamma) x z}{x^2 + \text{tg}^2(\gamma)(-t_1^2 + z^2)} \right) \\
& + x^4 \left(2 \ln \left(8x \sqrt{x^2 - \text{tg}^2(\gamma)(t_1 - z)^2} \right) + 6 \ln \left(x^2 \sqrt{x^2 - \text{tg}^2(\gamma)(t_1 - z)^2} \right) \right. \\
& - \ln \left(\text{tg}(\gamma) \sqrt{x^2 - \text{tg}^2(\gamma)(t_1 - z)^2} (t_1 + z) + \sqrt{-(\text{tg}(\gamma) t_1 + x - \text{tg}(\gamma) z)} \right. \\
& \left. \left. \sqrt{(-\text{tg}(\gamma) t_1 + x + \text{tg}(\gamma) z)(x - \text{tg}(\gamma)(t_1 + z))(x + \text{tg}(\gamma)(t_1 + z))} \right) \right) \\
& - 6 \ln \left(-2x \sqrt{x^2 - \text{tg}^2(\gamma)(t_1 - z)^2} \left(\text{tg}(\gamma)(t_1 + z) - \sqrt{-x^2 + \text{tg}^2(\gamma)(t_1 + z)^2} \right) \right) \\
& - \ln \left(-\sqrt{x^2 - \text{tg}^2(\gamma)(t_1 - z)^2} \left(\text{tg}(\gamma)(t_1 + z) + \sqrt{-x^2 + \text{tg}^2(\gamma)(t_1 + z)^2} \right) \right) \\
& - \text{tg}^2(\gamma) x^2 \left(-t_1 z \ln(4096) - 2(t_1 - z)^2 \ln \left(x \sqrt{x^2 - \text{tg}^2(\gamma)(t_1 - z)^2} \right) \right. \\
& + 6(t_1 - z)^2 \ln \left(x^2 \sqrt{x^2 - \text{tg}^2(\gamma)(t_1 - z)^2} \right) + t_1^2 \ln \left(\text{tg}(\gamma) \sqrt{x^2 - \text{tg}^2(\gamma)(t_1 - z)^2} \right. \\
& \left. (t_1 + z) + \sqrt{-(\text{tg}(\gamma) t_1 + x - \text{tg}(\gamma) z)(-\text{tg}(\gamma) t_1 + x + \text{tg}(\gamma) z)(x - \text{tg}(\gamma)(t_1 + z))} \right. \\
& \left. \sqrt{(x + \text{tg}(\gamma)(t_1 + z))} \right) - 2t_1 z \ln \left(\text{tg}(\gamma) \sqrt{x^2 - \text{tg}^2(\gamma)(t_1 - z)^2} (t_1 + z) \right. \\
& \left. + \sqrt{-(\text{tg}(\gamma) t_1 + x - \text{tg}(\gamma) z)(-\text{tg}(\gamma) t_1 + x + \text{tg}(\gamma) z)(x - \text{tg}(\gamma)(t_1 + z))} \right. \\
& \left. \sqrt{(x + \text{tg}(\gamma)(t_1 + z))} \right) + z^2 \ln \left(\text{tg}(\gamma) \sqrt{x^2 - \text{tg}^2(\gamma)(t_1 - z)^2} (t_1 + z) \right. \\
& \left. + \sqrt{-(\text{tg}(\gamma) t_1 + x - \text{tg}(\gamma) z)(-\text{tg}(\gamma) t_1 + x + \text{tg}(\gamma) z)(x - \text{tg}(\gamma)(t_1 + z))} \right. \\
& \left. \sqrt{(x + \text{tg}(\gamma)(t_1 + z))} \right) - 6t_1^2 \ln \left(-2x \sqrt{x^2 - \text{tg}^2(\gamma)(t_1 - z)^2} (\text{tg}(\gamma)(t_1 + z) \right. \\
& \left. - \sqrt{-x^2 + \text{tg}^2(\gamma)(t_1 + z)^2} \right) + 12t_1 z \ln \left(-2x \sqrt{x^2 - \text{tg}^2(\gamma)(t_1 - z)^2} \right. \\
& \left. \left(\text{tg}(\gamma)(t_1 + z) - \sqrt{-x^2 + \text{tg}^2(\gamma)(t_1 + z)^2} \right) \right) - 6z^2 \ln \left(-2x \sqrt{x^2 - \text{tg}^2(\gamma)(t_1 - z)^2} \right. \\
& \left. \left(\text{tg}(\gamma)(t_1 + z) - \sqrt{-x^2 + \text{tg}^2(\gamma)(t_1 + z)^2} \right) \right) + t_1^2 \ln \left(-64 \sqrt{x^2 - \text{tg}^2(\gamma)(t_1 - z)^2} \right. \\
& \left. \left(\text{tg}(\gamma)(t_1 + z) - \sqrt{-x^2 + \text{tg}^2(\gamma)(t_1 + z)^2} \right) \right)
\end{aligned} \tag{5.20}$$

$$\begin{aligned}
& \left(\operatorname{tg}(\gamma)(t_1 + z) + \sqrt{-x^2 + \operatorname{tg}^2(\gamma)(t_1 + z)^2} \right) + z^2 \ln \left(-64 \sqrt{x^2 - \operatorname{tg}^2(\gamma)(t_1 - z)^2} \right. \\
& \left. \left(\operatorname{tg}(\gamma)(t_1 + z) + \sqrt{-x^2 + \operatorname{tg}^2(\gamma)(t_1 + z)^2} \right) - 2t_1 z \ln \left(-\sqrt{x^2 - \operatorname{tg}^2(\gamma)(t_1 - z)^2} \right. \right. \\
& \left. \left. \left(\operatorname{tg}(\gamma)(t_1 + z) + \sqrt{-x^2 + \operatorname{tg}^2(\gamma)(t_1 + z)^2} \right) \right) \right) + \operatorname{tg}^4(\gamma) \left(-4(t_1 - z)^4 \right. \\
& \ln \left(x \sqrt{x^2 - \operatorname{tg}^2(\gamma)(t_1 - z)^2} \right) + 2(t_1 - z)^4 \ln \left(\operatorname{tg}(\gamma) \sqrt{x^2 - \operatorname{tg}^2(\gamma)(t_1 - z)^2} (t_1 + z) \right. \\
& \left. + \sqrt{-(\operatorname{tg}(\gamma)t_1 + x - \operatorname{tg}(\gamma)z)(-\operatorname{tg}(\gamma)t_1 + x + \operatorname{tg}(\gamma)z)(x - \operatorname{tg}(\gamma)(t_1 + z))} \right. \\
& \left. \sqrt{x + \operatorname{tg}(\gamma)(t_1 + z)} \right) + t_1 z \left(-2t_1 z \ln(64) + (t_1^2 + z^2) \ln(256) - 4(2t_1^2 - 3t_1 z + 2z^2) \right. \\
& \left. \ln \left(-2 \sqrt{x^2 - \operatorname{tg}^2(\gamma)(t_1 - z)^2} \left(\operatorname{tg}(\gamma)(t_1 + z) + \sqrt{-x^2 + \operatorname{tg}^2(\gamma)(t_1 + z)^2} \right) \right) \right) \\
& \left. + 2(t_1^4 + z^4) \ln \left(-\sqrt{x^2 - \operatorname{tg}^2(\gamma)(t_1 - z)^2} \left(\operatorname{tg}(\gamma)(t_1 + z) \right. \right. \right. \\
& \left. \left. \left. + \sqrt{-x^2 + \operatorname{tg}^2(\gamma)(t_1 + z)^2} \right) \right) \right] / \left(48 \operatorname{tg}(\gamma) \sqrt{x^2 - \operatorname{tg}^2(\gamma)(t_1 - z)^2} \right).
\end{aligned}$$

$$\operatorname{Intersection}(x, y, z) = \operatorname{IntersectionY}(\sqrt{x^2 + y^2}, t_1 - |z|). \quad (5.21)$$

Bibliography

- [1] Moller J., Waagepetersen R. P.: *Statistical Inference and Simulation for Spatial Point Processes*, Chapman & Hall/CRC, 2004.
- [2] Moller J., Ghorbani M.: Aspects of second-order analysis of structured inhomogeneous spatio-temporal point processes, In: *Statistica Neerlandica* 66, 4, 472-491, 2012.
- [3] Pawlas Z.: *Prostorové modelování, prostorová statistika 1*, Učební text MFF UK, Praha, 2010.
- [4] Prokešová M., Hellmund G., Jensen E.B.V.: On spatio-temporal Lévy based Cox processes, In: *Proceedings S⁴G International Conference on Stereology, Spatial Statistics and Stochastic Geometry*, Prague, Editors: Lechnerová R., Saxl I., Beneš V., Union of Czech math. and physicists, 111-116, 2006.

List of Figures

5.1	Realization of a point process from Model 1, Model 2 and Model 3. The vertical axis is temporal, the other two axis are spatial. . .	43
5.2	Model 1. First row: estimates of F function. Second row: (c) blue line is the real ρ_{time} function, red line is an estimate, (d) blue surface is the real ρ_{space} function, green surface is an estimate. Third row: red dots are estimates of K_1 (f) and K_2 (e) functions using estimate of intensity function, green dots are estimates using the theoretical intensity function, blue line is function $2t$ (e) and πr^2 (f).	44
5.3	Model 2. First row: black dots are real K_2 (a) and K_1 (b) functions, green dots are estimates of K_2 (a) and K_1 (b) functions, red dots are estimates using estimate of intensity function, blue line is function $2t$ (a) and πr^2 (b). Second row: (c) estimate of F function using real intensity function, (d) estimate of F function using estimate of intensity function. Third row: theoretical F function.	45
5.4	Model 3. First row: black dots are real K_2 (a) and K_1 (b) functions, green dots are estimates of K_2 (a) and K_1 (b) functions, red dots are estimates using estimate of intensity function, blue line is function $2t$ (a) and πr^2 (b). Second row: (c) estimate of F function using real intensity function, (d) estimate of F function using estimate of intensity function. Third row: theoretical F function.	46
5.5	K function for Model 1 (a), for Model 2 (b) and for Model 3 (c). For each figure, there are three surfaces. Black surface is the theoretical K function (for the corresponding model with numerically specified parameters), green surface is the estimated K function using the theoretical intensity function and red surface is the estimated K function using the estimated intensity function.	47
5.6	Pair correlation functions for Model 1 (a) for Model 2 (b) and for Model 3 (c) (with numerically specified parameters) as a function of time and the distance from the origin in the spatial coordinate. Values in point $(0, 0)$: (a) $\tilde{g}(0, 0) \doteq 168$, (b) $\tilde{g}(0, 0) \doteq 287$, (c) $\tilde{g}(0, 0) \doteq 1669$	47

List of Tables

5.1	Sum of square errors for intensity function estimate from 100 simulations.	40
-----	--	----